Charles University in Prague

Faculty of Science

Study programme: Biology

Curriculum: Cell and Developmental Biology – Cell Physiology

Bc. Terezie Imrichová

The response of metastatic prostate cancer cell lines to genotoxic stress

Odpověď metastatických buněčných linií karcinomu prostaty na genotoxický stres

Diploma thesis

Supervisors: Zdeněk Hodný, MD, Ph.D.; Robert Strauss, Ph.D.

Prague, 2013

I hereby declare that I completed this master thesis independently under the guidance of Zdeněk Hodný, MD, Ph.D. and Robert Strauss, Ph.D. It documents my own work if not explicitly otherwise mentioned. I have properly acknowledged and cited all sources used. The thesis is not subject of any other defending procedure.

Prague, August 10 2013 .....

Acknowledgements

In the first place I would like to thank my supervisor, Zdeněk Hodný, MD, Ph.D., for admitting me to the Genome Integrity Unit of the Institute of Molecular Genetics, for his valuable comments to this thesis and for allowing me to conduct a part of my experimental work at Danish Cancer Society Research Center, Copenhagen, Denmark.

I would also like to thank Mgr. Lenka Kyjacová, a postgradual student in our research group, for her plentiful help and advice.

Many thanks belong to Prof. Jiří Bartek, MD, Ph.D., the head of Genome Integrity Unit of Danish Cancer Society Research Center, for accepting me into his excellent team and giving me the opportunity to gain a great life and scientific experience there.

Another big ackowledgement belongs to Robert Strauss, Ph.D., a junior scientist in the Genome Integrity Unit who supervised my work there, for the time he spent with my project, for his patience and many useful advice. Equally I would like to express my thanks to Mgr. Jitka Ostraková and other members of the Genome Integrity Unit for being very kind and helpful during my stay in the laboratory.

Last but not least, I would like to thank my family and my boyfriend for their love and support during my whole studies.

Abstract

Prostate cancer is the fourth most frequent cause of cancer-related deaths in men worldwide. One of current successful approaches to treat prostate cancer is radical prostatectomy followed by radiotherapy. However, this treatment is not 100% successful, as 53% patients develop secondary tumors. Our hypothesis is, that ionizing radiation itself contributes to the development of metastases by inducing changes in cell phenotype, particularly in terms of epithelial-to-mesenchymal transition and stemness. To test this hypothesis, we irradiated the cells of metastatic prostate cancer cell line DU145 by fractionated radiation 2 x 10 Gy and we compared the expression of selected epithelial, mesenchymal and stem-cell markers prior to and after irradiation. Besides we focused on a subpopulation of so called floating cells which arise during irradiation. These cells can survive the radiation treatment and after some time they are able to reattach and give rise to readherent population. We wanted to asses what is the cell cycle profile of these cells and whether and how fast they proliferate.

In this thesis we have shown that radiation causes only minor changes in epithelial/mesenchymal and stem-like character of adherent fraction of the DU145 cell line. However, we have also described that small population of cells is able to survive radiation treatment and to detach from the surface and surrounding tissue without anoikis. These floating cells remain arrested in G2/M phase for several weeks whereupon they reattach and restart proliferation. Further experiments are needed to determine whether these cells can give rise to secondary tumors *in vivo*.

Key words:

ionizing radiation, radioresistance, DU145, prostate cancer, epithelial-to-mesenchymal transition, stem cells, non-adherent cells, cell cycle arrest

Abstrakt

Rakovina prostaty je u mužů čtvrtá nejčastější příčina úmrtí v oblasti nádorových onemocnění. Jedním z nejúčinnějších léčebných přístupů je v současnosti radikální prostatektomie následovaná terapeutickým ozařováním. Tato metoda však není stoprocentně účinná; až u 53 % pacientů se po ozařování objeví sekundární nádory. Dle naší hypotézy samo ionizující záření indukuje v buňkách změny, týkající se zejména epiteliálně-mesenchymální tranzice a kmenovosti, které umožňují nádoru metastázovat. Abychom tuto hypotézu ověřili, ozařovali jsme buňky metastatické nádorové linie rakoviny prostaty DU145 frakcionovaným zářením 10 x 2 Gy a sledovali jsme expresi vybraných epiteliálních, mezenchymálních a kmenových markerů před a po ozáření. Kromě toho jsme se zaměřili na subpopulaci tzv. plovoucích buněk, které vznikají během ozařování. Tyto buňky jsou schopny přežít ozařovací režim, po nějaké době přisednou zpět na podklad a dají vzniknout readherentní populaci. Naším cílem bylo stanovit, v jaké fázi buněčného cyklu se tyto buňky nacházejí a zda, příp. jak rychle proliferují.

V této práci jsme ukázali, že ozařování působí jen malé změny týkající se epiteliálního/mesenchymálního a kmenového charakteru adherentní frakce DU145 buněk. Dále jsme experimentálně prokázali, že malá populace buněk je schopná přežít proces ozařování a odpoutat se od kultivačního povrchu nebo/a okolních buněk, aniž by podlehla anoikis. Tyto buňky jsou po několik týdnů zastaveny v G2/M fázi, načež adherují a začnou znovu proliferovat. Je třeba dalších experimentů, abychom byli schopni určit, zda jsou tyto buňky schopny tvořit sekundární nádory *in vivo*.

Klíčová slova:

ionizující záření, radioresistence, DU145, rakovina prostaty, epiteliální-mesenchymální transice, kmenové buňky, plovoucí buňky, zástava buněčného cyklu

Contents

1. Introduction 9
1.1. The prostate 9
1.2. Prostate cancer 10
1.3. Prostate cancer cell lines....12
1.4. Epithelial to mesenchymal transition 14
1.5. Prostate cancer treatment and radioresistance 19
1.6. Previous achievements and project description....23
2. Materials and methods 27
2.1. Introduction to the methods 27
2.1.1. Ionizing radiation....27
2.1.2. Immunofluorescence 28
2.1.3. Flow cytometry 28
2.1.4. Cell cycle analysis by flow cytometry....29
2.1.5. Cell proliferation dye....30
2.2. Materials and methods for this project 30
2.2.1. Cell line and culture....30
2.2.2. Irradiation of cells and obtaining fractions 31
2.2.3. Immunofluorescence 31
2.2.4. FACS analysis – mesenchymal and stem cell markers 32
2.2.5. FACS analysis – cell proliferation 32
2.2.6. FACS analysis – cell cycle profile 33
3. Results 35
3.1. Expression of selected epithelial, mesenchymal and stem cell antigens in control cells 35
3.2. Cell survival and cell floating after irradiation 37
3.3. Expression of selected mesenchymal markers after irradiation....39
3.4. Expression of selected mesenchymal and stem cell markers decreases in floating cell fraction, but ionizing radiation seems to counteract this process 40
3.5. Radiation causes cell cycle arrest....44
3.6. Cell cycle profile of irradiated cells 46
3.7. Irradiated floating cells need to readhere to restart proliferation....48
3.8. Vimentin and E-cadherin expression in readherent cells 50
3.9. E-cadherin, CD44 and CD49f expression in readherent cells estimated by flow cytometry .50
4. Discussion....53

4.1. Expression of selected epithelial, mesenchymal and stem cell markers in control cells.....53
4.2. Expression of selected mesenchymal and stem cell markers decreases in floating cell fraction, but ionizing radiation seems to counteract this process 55
4.3. Radiation causes cell cycle arrest in G2/M phase.....56
4.4. Expression of selected epithelial, mesenchymal and stem cell markers in readherent cells58
5. Conclusion.....60
6. Resources.....61

List of abbreviations

Akt	protein kinase B; RAC serine/threonine-protein kinase
APC	adenomatous polyposis coli
APC	allophycocyanin
AR	androgen receptor
ATM	ataxia telangiectasia mutated
ATR	ataxia telangiectasia and Rad3-related protein
Bcl-2	B-cell lymphoma 2
bHLH	basic helix-loop-helix
Bmi1	B lymphoma Mo-MLV insertion region 1 homolog
BRAF	*v-raf murine sarcoma viral oncogene homolog B1, rapidly accelerated fibrosarcoma*
CADM2	cell adhesion molecule 2
CaP	prostate carcinoma
CD44	cluster of differentiation 44
CD49f	cluster of differenntiation 49f, integrin α6
CD133	cluster of differentiation 133
Chk1	checkpoint kinase-1
Chk2	checkpoint kinase-2
CK	cytokeratin
CSCs	cancer stem cells
CTRL	control
DAB2IP	DAB2 interacting protein
DAPI	4',6-diamidino-2-phenylindole
dEF1	elongation factor 1-delta
DMEM	Dulbecco's modified Eagle's medium
DNA	deoxyribonucleotic acid
DNA-PK	DNA-dependent protein kinase (catalytic subunit)
DVL2	dishevelled 2
E2α	transcription factor E2-alpha
E47	immunoglobulin enhancer-binding factor E12/E47
EMT	epithelial-to-mesenchymal transition
ERG	*Ets-related gene*
Erk	extracellular signal-regulated kinase
EZH2	enhancer of zeste homolog 2
FACS	fluorescence activated cell sorting
FBS	fetal bovine serum
FOXC2	forkhead box protein C2
FOXP1	*forkhead box protein P1*
GADD45A	growth arrest and DNA damage-inducible protein GADD45 alpha
Gli-1	zinc finger protein GLI-1, glioma-associated oncogene
GSK-3β	glycogen synthase kinase 3 beta
HEY1	hairy/enhancer-of-split related with YRPW motif protein 1
HIF-1α	hypoxia-inducible factor 1-alpha
HMEC	human mammary epithelial cells

ILK	integrin linked kinase
JAK	Janus kinase
KLF8	Krueppel-like factor 8
KRAS	*V-Ki-ras2 Kirsten rat sarcoma viral oncogene homolog*
MAGI2	membrane associated guanylate kinase, WW and PDZ domain containing 2
MAPK	mitogen activated protein kinase
Mdm2	mouse double minute 2, E3 ubiquitin-protein ligase
MET	mesenchymal-to-epithelial transition
miR	micro RNA
MMP 2, 3, 9	matrix metalloproteinase-2, 3, 9
mRNA	messenger RNA
mTOR	mammalian target of rapamycin
NCOA2	nuclear receptor coactivator 2
NF-κB	nuclear factor kappa B
Nkx3.1	*NK homeobox (Drosophila), family 3, A*
Notch	neurogenic locus notch protein homolog
p27	protein p27kip1
p53	protein 53 (TP53)
p63	protein 63, p53 homolg
Par6	partitioning defective protein 6
PARP	poly [ADP-ribose] polymerase
PI3K	phosphatidylinositol 3' -kinase
PIK3CA	*phosphatidylinositol-4,5-bisphosphate 3-kinase, catalytic subunit alpha*
PTEN	phosphatase and tensin homolog
Raf	RAF proto-oncogene serine/threonine-protein kinase, rapidly accelerated fibrosarcoma
Ras	Ras (rat sarcoma) protein
RNA	ribonucleotic acid
RT	radiation therapy
SA-βgal	senescence-associated beta-galactosidase
SIP1	survival of motor neuron protein-interacting protein 1
SMAD	small mothers against decapentaplegic, SMAD family member
Sox-10	SRY (sex determining region Y)-box 10
STAT	signal transducer and activator of transcription
TCF/LEF	T cell transcription factor/lymphoid enhancer-binding factor
TCF4/ITF2	T cell transcription factor 4/Immunoglobulin transcription factor 2
TCF-8	T cell transcription factor 8
TFs	Transcription factors
TGF-β	transforming growth factor beta
TMPRSS2	*transmembrane protease, serine 2*
TP53	tumor protein 53 (p53)
Wee1	Wee1-like protein kinase
Wnt	Wingless type (Wnt protein)
XRCC4	X-ray repair cross-complementing protein 4
ZEB1, 2	zinc finger E-box-binding homeobox 1, 2
ZFXH1B	zinc finger homeobox protein 1b

1. Introduction

1.1. The prostate

1.1.1. Prostate gland

Prostate gland is a single donut-shaped gland below the bladder and surrounding the upper part of the urethra. It is the largest among the accessory sex structures, comprised of 30 to 50 tubuloalveolar glands. The prostatic acini are lined by an epithelium embracing columnar cells of various shapes and sizes and also basal cells. Together with seminal vesicles it secretes the bulk of the fluid in which ejaculated sperms are suspended. This fluid contains number of products such as citric acid, acid phosphatase or prostate-specific antigen. The main function of prostate is to contribute to the volume of semen and to provide a transfer medium for the spermatozoa into female tract. The function of prostate is decisively controlled by androgens. Withdrawal of androgens is accompanied by involution and atrophy of the gland and a cessation or marked decline of its secretory activity (Greger and Windhorst 1996, Vander et al. 1990).

1.1.2. Human prostate epithelium

Glandular epithelium of normal prostate is composed of four cell types: basal, neuroendocrine, luminal and intermediate (transit amplifying).

The basal cells form a layer along the basement membrane of each prostatic duct, with cytokeratins CK5 and CK14, the cell-surface marker CD44 (van Leenders et al. 2000), the p53 homologue p63 (Signoretti et al. 2000) and the anti-apoptotic protein Bcl-2 (Long et al. 2005) being the most common markers used to characterize them.

Neuroendocrine cells also reside along the basement membrane and secrete neuroendocrine peptides that support epithelial growth and viability. They can be identified according to expression of neuron-specific enolase and neuropeptides, like chromogranin A (Huttner et al. 1991).

Luminal cells form a layer just above the basal cells and secrete prostatic proteins into the luminal space. Their typical markers are cytokeratins CK8 and CK18, the cell-surface marker CD57 (Long et al. 2005) and prostate-specific antigen (Bonkhoff et al. 1996). The androgen receptor (AR) and the *Nkx3.1* gene *(NK homeobox (Drosophila), family 3, A* gene*)* are also preferentially, but not exclusively, expressed in the luminal cells (Isaacs et al. 1989, Bhatia-Gaur 1999).

Traditionally, basal and luminal cells were considered two distinct cell types. However, during differentiation process some cells migrate from the basal to the luminal layer, transforming from the early progenitor basal cells to the terminally differentiated secretory cells (Verhagen et al. 1988, van Leenders et al. 2000). These migrating cells express both basal and luminal cell markers and are therefore termed “intermediate cells” or “transit amplifying cells”. Phenotypically, they are very heterogeneous and their only specific marker seems to be cytokeratin CK19 (Long et al. 2005).

1.2. Prostate cancer

Prostate carcinoma (CaP) is the most prevalent cancer in men with the second highest incidence and the sixth highest mortality worldwide. Although the rates vary widely between countries, it is least common in South and East Asia, more common in Europe, and most common in the United States, especially in Afroamerican population. It develops primarily in men over fifty and almost all men aged 80 years show at least some microscopic evidence of it. In the Czech Republic CaP has the highest incidence and prevalence, as well as the third highest mortality among all cancers in men (http://globocan.iarc.fr).

1.2.1. Prostate cancer phenotype

More than 95% of prostate tumors are adenocarcinomas, however, some other rare variants have been identified during the past twenty years. Among them we can find some special epithelial tumors, mesenchymal, neuroendocrine and stromal tumors or tumors of haematolymphoid origin such as lymphoma or leukaemia (Chang et al. 2008).

Traditionally, prostate adenocarcinoma was thought to originate from luminal cells of the prostate epithelium, as expression of luminal cell markers, such as CK8 and CK18 as well as prostate-specifice antigen secretion have often been detected in the tumors. Loss of the expression of the basal cell antigens (CK5, CK14, p63) and luminal cells expansion have actually served as diagnostic criteria for CaP for a long time (Humphrey et al. 2007).

On the other hand, most of castrate-resistant CaPs express basal cell characteristics, such as the expression of Bcl-2 or androgen independence, which are not merely markers, but actively contribute to the castrate-resistant phenotype (McDonnell et al. 1992). What is more, many experiments have shown that transformed basal cells can give rise to tumors that are composed of cells displaying a luminal cell phenotype (Goldstein et al. 2010, Min et al. 2010, Taylor et al. 2012),

which supports the hypothesis that CaP has its origin in basal cells. Finally, the third type of prostate epithelial cells, intermediate cells, have also been observed in human CaP tissues in some reports (Verhagen et al. 1992).

Contemporary, the leading hypothesis is that both basal and luminal cells have the potential to develop CaP, but basal cells need to trans-differentiate into the luminal cell type first (Choi et al. 2012, Xin 2013). During the transdifferentiation process intermediate cells can be detected.

1.2.2. Normal and cancer stem cells in the prostate

There are two types of cells important for CaP initiation and regeneration: the cell(s) of origin and cancer stem cell(s). Whereas the cell of origin is characterized as a cell that serves as target for transformation during tumor initiation, cancer stem cells (CSCs) represent the cellular subfractions that can repeatedly regenerate the tumor. These two types of cells may but does not have to be of identical origin.

As mentioned above, the cells of origin are now supposed to reside in the basal cell layer. CSCs, on the contrary, still have not been satisfyingly characterized. It is not even clear, whether they originate from normal prostate stem cells or whether they can arise from any cell of the prostate epithelium. Some experiments suggest that normal and cancer prostate stem cells do not represent the same population but are actually two different cell types (Taylor et al. 2012). Others, however, believe, that CSCs are in fact transformed normal stem cells. Therefore, it is crucially important to understand the nature of normal prostate stem cells.

The preferential survival of basal cells following androgen ablation has led to the traditionally held hypothesis of prostate stem cells, which are supposed to reside within the basal cell layer of the gland (English et al. 1987). However, 5-bromo-2'-deoxyuridine pulse chase experiments performed by Tsujimura et al. (Tsujimura et al. 2002) show that both basal and luminal cells in a specific region proximal to the urethra retain the label after many cycles of androgen ablation and add-back. These cells possess enhanced growth activity, and are able to self-renew to regenerate prostate tissue de novo (Tsujimura et al. 2002, Goto et al. 2006). Finally, cells of luminal phenotype have been recently proposed as the cells of origin in the human CaP xenograft BM18 (Germann et al. 2012).

1.2.3. Prostate cancer genetics

Even though it is important to know in which cell CaP originates, it is even more important to decipher what are the genomic events enabling its transformation. Two integrative analyses performed in 2010 and 2011 identified many new mutations in gene coding regions as well as other genomic rearrangements involved in CaP initiation and progression, and supplemented the information we had from previous experiments.

For example, recurrent gene fusions have been spotted between androgen-regulated genes and genes for the family of the E26 transformation-specific transcription factors. These findings suggest that genomic rearrangements may represent a major mechanism driving prostate carcinogenesis (Tomlins et al. 2007). In addition, the androgen-driven *TMPRSS2-ERG* fusion was associated with a previously unrecognized, prostate-specific deletion at chromosome 3p14, which implicates here located genes *FOXP1 (forkhead box P1), RYBP (ring finger protein 1 and YY1 transcription factor binding protein),* and *SHQ1 (Small nucleolar RNAs of the box H/ACA family Quantitative accumulation 1)* as potential cooperative tumor suppressors (Taylor et al. 2010).

In the most integrative analysis of CaP genome focusing on gene-coding regions, *nuclear receptor coactivator 2* (*NCOA2)* was identified as an oncogene in ~11% of tumors. It was further discovered, that mutations in commonly mutated oncogenes and tumor suppressor genes such as *PIK3CA, KRAS, BRAF, and TP53* are present but rare, whereas changes in the PI3K, Ras/Raf, and androgen receptor (AR) pathways were found in nearly all metastatic samples and in a large fraction of primary samples (Taylor et al. 2010). A few additional mutations were found in a whole-genome-sequencing study by Berger et al. Namely they were rearrangements disrupting genes for CADM2 (cell adhesion molecule 2, cell polarity maintenance molecule and a putative tumor suppressor), PTEN (phosphatase and tensin homolog), or MAGI2 (PTEN interacting protein; Berger et al. 2011).

1.3. Prostate cancer cell lines

Over the years, cells from prostate carcinoma have proven to be one of the most difficult cell types from which to establish continuous cell lines. Approximately 30 putative human prostate cell lines have been described and used for research purposes from 1970 to the present. However, it was shown recently, that only 17 of them are unique in origin or independently established from the same patient and/or sources, whereas the others are related in origin or derivative of other cell lines (van Bokhoven et al. 2003). The three earliest established CaP cell lines, DU145, PC-3 and LNCaP are

the most commonly used models for in vitro studies. Although the two first lines express some mesenchymal cell markers, all the three lines are characterized as epithelial (https://www.atcc.org).

Personally, I have been working with DU145 and PC-3 cells, hence I would like to characterise these two cell lines here.

1.3.1. DU145

The DU145 cell line was established in 1977 (Stone et al. 1978). Originally it comes from brain metastasis and it has been demonstrated to have no AR either on mRNA or on protein level. When p53 status of this line was examined, two mutations in exons 6 and 8 were found, both of them resulting in an amino-acid change on protein level (so called missense mutation) affecting DNA binding domain of p53 and its transcriptional activity.

Focusing on some epithelial and mesenchymal cell markers, the DU145 cell line was found to express CK5 (epithelial basal cell marker), CK8 and CK18 (epithelial luminal cell markers, van Bokhoven et al. 2003), E-cadherin (epithelial cell marker), catenins α, β and γ (cytoplasmic proteins important for downstream cadherin signalling, Murali et al. 2012), as well as one mesenchymal cell marker, extracellular matrix protein vimentin (van Bokhoven et al. 2003). Despite E-cadherin expression, DU145 cells were found to be somewhat invasive in an in vitro invasion assay (Murali et al. 2012). They produce poorly differentiated tumors if inoculated into nude mice (Russel et al. 2003).

1.3.2. PC-3

The second cell line, PC-3, was established in 1978 (Kaighn et al. 1979). It originates from bone metastasis and shows no presence of AR on mRNA or protein level, thus being androgen independent. It harbors a frameshift mutation in exon 5 of p53 gene resulting in STOP codon (so called nonsense mutation) in both alleles; consequently p53 translation is terminated prematurely and no protein can be detected.

The PC-3 cells express the same epithelial markers as DU145 (CK5, CK8 and CK18, van Bokhoven et al. 2003; E-cadherin, Murali et al. 2012), moreover, the expression of neuron-specific enolase, an enzyme characteristic for neuroendocrine cells of prostate epithelium, was detected. On the other hand, they express more mesenchymal markers than DU145: vimentin (van Bokhoven 2003), N-cadherin and cadherin 11 (Murali et al. 2012). Only two catenins, β and γ, were found in these cells (Murali et al. 2012). However, the gain of expression of mesenchymal markers seems

insufficient for an invasive phenotype in vitro. In fact, the PC-3 cells were even less invasive than DU145 in the in vitro invasion assay (Murali et al. 2012). They also produce poorly differentiated tumors if inoculated into nude mice (Russel et al. 2003).

1.4. Epithelial to mesenchymal transition

Epithelial and mesenchymal cells represent distinct lineages, each with a unique gene expression profile and cell morphology.

1.4.1. Epithelial phenotype

Epithelial cells usually grow in one continuous layer with regularly distributed cell-cell junctions and adhesions between neighbouring cells. There are four major types of cell-cell junctions: tight junctions, adherens junctions, hemidesmosomes and gap junctions; the first two of them being the most important for maintaining the epithelial character of the tissue. These junctions hold the cells tightly together and inhibit the movement of individual cells. Furthermore, they result in barrier function of epithelial cell layer and allow the asymmetrical distribution of cell membrane phospholipids and proteins, which leads to apicobasal polarization of the whole epithelial sheet (Lee et al. 2006).

1.4.2. Mesenchymal phenotype

Mesenchymal cells do not exhibit such an organized structure as epithelial cells, neither they possess tight intracellular junctions. They tend to form structures of irregular shape with non-uniform composition or density. Adhesions between mesenchymal cells are less strong than in their epithelial counterparts, allowing for increased migration. Moreover, mesenchymal migration is mechanistically different from epithelial movement. Epithelial cells move as one sheet, whereas mesenchymal cells move individually and can leave part of the region behind. Mesenchymal cells also have a more extended and elongated shape and they have characteristic front-to-back leading edge polarity. Unlike epithelia, the irregular structure of mesenchyme does not much allow for topological specialization (Lee et al. 2006).

1.4.3. Transition between the phenotypes

Epithelial cells can convert into mesenchymal cells by a process known as the epithelial–mesenchymal transition (EMT). During EMT epithelial cells lose many of their epithelial characteristics and adapt properties that are typical for mesenchymal cells. This requires complex changes in cell architecture and behaviour, some of which are listed in Table 1. However, not all of the inter- and intracellular changes are always seen during EMT. The precise spectrum of changes that actually occur is probably determined by the integration of extracellular signals the cell receives, although this is still unclear (Thiery and Sleeman 2006).

EMT and reverse mesenchymal-epithelial transition (MET) play an important role in many physiological processes, such as embryonic development, tissue regeneration, cancer progression or maintenance of stem cell properties (Strauss et al. 2012). In cancer, EMT allows the cell to overcome the constraints imposed on it by intercellular junctions and adopt a motile phenotype to invade surrounding tissues and metastasize.

Proteins that increase in abundance	**Proteins that decrease in abundance**	**Proteins that accumulate in the nucleus**	**Proteins whose activity increases**	**In vitro functional markers**
N-cadherin	E-cadherin	β-catenin	ILK	Increased migration
Vimentin	Desmoplakin	Smad-2/3	GSK-3β	Increased invasion
Fibronectin	Cytokeratin	NF-κβ	Rho	Increased scattering
Snail1 (Snail)	Occludin	Snail1 (Snail)		Elongation of cell shape
Snail2 (Slug)		Snail2 (Slug)		Resistance to anoikis
Twist		Twist		
Goosecoid				
FOXC2				
Sox10				
MMP-2				
MMP-3				
MMP-9				
Integrin αvβ6				

Table 1: EMT markers (according to Lee et al. 2007)

1.4.4. EMT induction and accomplishment

1.4.4.1. Extracellular signals

There are number of extracellular signals regulating EMT:

- Transforming growth factor β (**TGF-β**) signalization – comprises signalling through SMAD transcription factors; phosphorylation of partitioning defective protein 6 (Par6) and occludin leading to a loss of tight junctions and apical-basal polarity (Ozdamar et al. 2005); and collaboration with Wnt, Notch, and receptor tyrosine kinase signals (Grünert et al. 2003).
- **Wnt** signalization
    - canonical – Wnt proteins bind to cell-surface receptors of the Frizzled family, causing the receptors to activate Dishevelled family proteins and ultimately resulting in a change in the amount of β-catenin, that reaches the nucleus. Other proteins, such as axin, GSK-3β, APC (adenomatous polyposis coli) and TCF/LEF transcription factors, are involved.
    - non canonical – e.g. planar cell polarity or Wnt/calcium pathways (Yang and Weinberg, 2008)
- **Notch** signalization – involves Notch ligands Delta/Jagged, cooperates with TGF-β signalling (Huber et al. 2005).
- Signalization from **tyrosine kinase receptors** – receptor for hepatocyte growth factor, fibroblast growth factor receptor, insulin-like growth factor 1 receptor, epidermal growth factor receptor and platelet-derived growth factor receptor family members; and their downstream substrates (Yang and Weinberg 2008). Important players in these pathways are e.g. Ras, PI3K/Akt, Raf/MAPK and others.
- **Hedgehog** signalization – with its downstream transcription factor Gli-1 (Huber et al. 2005).

Above that, EMT can be induced by other signals, e.g. E-cadherin loss by other reasons than diminished gene epression (Onder et al. 2008) or cell binding to collagen (Imamichi et al. 2007) and hyaluronan (Zoltan-Jones et al. 2003).

1.4.4.2. Transcription factors involved in EMT

The common terminal goal of the above mentioned signalling cascades is to activate transcription factor that regulates the expression of some key epithelial or mesenchymal genes.

Apart from the pathway-specific transcription factors, such as β-catenin, SMADs etc., there are also TFs, which are activated by more than one pathway and are tightly bound to the EMT process. These are above all the TFs regulating E-cadherin expression.

- **TFs directly repressing E-cadherin:**
    - zinc-finger TFs binding to E-boxes of the E-cadherin promoter: Snail1 (Snail; Batlle et al. 2000, Cano et al. 2000), Snail2 (Slug, Hajra et al. 2002), ZEB1 (dEF1, TCF-8; Eger et al. 2005), ZEB2 (SIP1, ZFXH1B; Comijn et al. 2001), KLF8 (Wang et al. 2007)
    - basic helix-loop-helix (bHLH) TFs binding to E-boxes of the E-cadherin promoter: E47 (E2α, Perez-Moreno et al. 2001), HEY1/2 (Lee et al. 2006).
- **TFs indirectly repressing E-cadherin:**
    - basic helix-loop-helix (bHLH) TFs: Twist1 (Yang et al. 2004), E2-2 (TCF4/ITF2, Sobrado et al. 2009)
    - other TFs: FOXC2 (Mani et al. 2007), Goosecoid (Hartwell et al. 2006)

Although main function of most of the above mentioned transcription factors is to regulate transcription of the E-cadherin gene, many of them participate in regulating other genes related to EMT. More recent studies have found that ZEB1, Snail, and Slug are capable of repressing the transcription of several polarity factors (Aigner et al. 2007, Spaderna et al. 2008). Furthermore, some of the pathway-specific TFs are able to induce or repress expression of the typical EMT TFs. β-catenin, for example, seems to induce transcription of Slug (Conacci-Sorrell et al. 2003) and Twist1 (Onder et al. 2008). Another example is NF-κB, which upregulates Twist and Snail TFs (Kang et al. 2004, Bachelder et al. 2005) thereby contributing to the EMT program.

1.4.4.3. Important members of the signaling chains

- Nuclear factor κB (**NFκB)** – TGF-β and Ras pathways exert their effects at least partly through NF-κB activity, with possible downstream targets Snail and Twist (Huber et al. 2004).
- Glycogen synthase kinase 3 β (**GSK3β**) – apart from targeting β-catenin for degradation, it has been found to downregulate Snail on both transcriptional and post-translational level (Bachelder et al. 2005, Zhou et al. 2004).
- Members of STAT family (**STAT3, STAT5**) – there are numerous links between STAT activation, E-cadherin downregulation and EMT (Colomiere et al. 2009, Yamashita et al. 2004 etc.).
- Dishevelled protein 2 (**DVL2**) – target of HEY1 (Notch pathway), represses the expression of Notch, GSK-3β and β-catenin (Zavadil et al. 2004).

- Matrix metalloproteinase-3 (**MMP3**) – induces alternative splicing, production of reactive oxygen species and activation of Snail1 (Radisky et al. 2005).
- Integrin linked kinase (**ILK**) – putative Snail activator, functions through poly (ADP-ribose) polymerase 1 (PARP1)-dependent mechanism (McPhee et al. 2008).
- EMT-regulating small non-coding RNAs – especially the ***miR-200* family**, which target the TFs ZEB1 and ZEB2, *miR-205* (Gregory et al. 2008), *miR10b* (Ma et al. 2007) and *miR-335* (Tavazoie et al. 2008).

1.4.5. EMT and stemness

There are several studies suggesting that EMT is tightly bound to stemness. For example, it has been shown that Snail1 and Twist1 are able to induce a stem-like stage in immortalized human mammary epithelial cells (HMEC, Mani et al. 2008). Twist1 has also been found to directly regulate expression of Bmi1, a polycomb-group protein involved in cell self-renewal. Twist1 and Bmi1 seem to further cooperate to induce EMT program in head and neck squamous cell carcinoma cell lines (Martin and Cano 2010). In addition, it has been shown using a mammary tumor progression model that cells possessing both stem and tumorigenic characteristics can be derived from HMEC following the activation of the Ras-MAPK pathway. The acquisition of stem and tumorigenic characteristics is driven by EMT induction (Morel et al. 2008). Last but not least, EMT and stemness has been induced in HMEC by receptor activator of NF-κB (RANK) overexpression recently (Palafox et al. 2012).

Another study on trophoblast stem cells showed that these cells are locked in an E/M hybrid stage after the controlled induction of EMT (Abell et al. 2011). Analogically, ovarian CSCs and progenitors simultaneously harbor epithelial and mesenchymal characteristics. This E/M hybrid stage seems to be crucially important for stem-like state maintenance, since clonal cultures that were restricted to either epithelial or mesenchymal phenotype were no more tumorigenic (Strauss et al. 2011).

Several authors have contributed to the explanation of the hybrid stage maintenance. In particular, Brabletz and Brabletz, suggested a mechanism in which fine balance between the ZEB transcription factors ZEB1 and ZEB2 (EMT activators) and members of the *miR-200* family (epithelial inducers) is needed to control the state of cancer stem cells (Brabletz and Brabletz 2010).

1.4.6. EMT in prostate cancer

Several studies have demonstrated the importance of EMT in CaP progression. For instance, switch from E-cadherin to N-cadherin in CaP samples is strongly associated with poor prognosis (Gravdal et al. 2007). Moreover, increased levels of EZH2 protein, which is known to mediate transcriptional silencing of E-cadherin by trimethylation of histon H3 lysine 27, have been observed in aggressive prostate solid tumors (Cao et al. 2008). Finally, the expression pattern of selected EMT markers was analysed in huge number of localized CaP samples. Among 13 examined markers, E-cadherin, Snail1, Twist and vimentin appeared to be closely associated with commonly used prognostic factors, when their high expression it the tumor indicated poor prognosis of the disease (Benshawy et al. 2013).

The EMT process was further investigated in vitro. Primary prostate epithelial cells immortalized by human telomerase reverse transcriptase were shown to undergo EMT spontaneously after 12 weeks of culturing. The new, mesenchymal-like cell line expressed lower levels of epithelial markers E-cadherin, CK14, CK5 and p63, whereas mesenchymal markers like N-cadherin, cadherin11, vimentin and fibronectin, as well as mesenchymal inducers Twist2 and Zeb1, were upregulated in these cells (Ke et al. 2008).

1.5. Prostate cancer treatment and radioresistance

1.5.1. Treatment of localized prostate cancer

CaP is diagnosed on the basis of clinical and pathological examination. After ascertaining the stage of the disease, a clinical decision has to be made, how to treat the specific patient. The key regulators of CaP therapy are clinical practice guidelines, the aim of which is to help physicians with clinical decision-making and to improve patient management and care. In Europe, the guidelines most relevant to CaP management are those of the European Association of Urology, however, some countries within Europe also have their own clinical guidelines for CaP diagnosis and treatment (Wolff et al. 2012). Usually localized disease is cured using one or more of the below listed methods.

- Radical prostatectomy – an operation which removes the entire prostate gland and seminal vesicles. It can be open, laparoscopic or robot-assisted (Dunn et al. 2011).
- Cryotherapy – involves in situ freezing by applying extremely cold temperature to destroy tumor tissue (Mouraviev et al. 2006).

- Radiation therapy (radiotherapy) – delivery of a curative dose of radiation to the prostate without damaging surrounding tissues (Aneja et al. 2012).

1.5.2. Advanced prostate cancer and its treatment

Advanced CaP refers to recurrent CaP on either systemic or local level following definitive therapy. Its treatment comprises:

- Hormone therapy – androgen deprivation therapy which, unfortunately, usually leads to castration-resistant phenotype development (Attard et al. 2006).
- Chemotherapy
    - standard combination of docetaxel (tubulin-stabilizing drug) and prednison (synthetic glucocorticoid stimulating apoptosis in sensitive tumor cells; Dunn et al. 2011).
    - novel tubulin-stabilizing drug cabazitaxel, combined with prednisone (Sartor et al. 2012)
    - targeted chemotherapeutics (Agarwal et al. 2012, Sartor et al. 2012, Amaral et al. 2012)
- New emerging therapies (Ouard 2013)

1.5.3. Focused on radiation therapy

1.5.3.1. Different forms of radiation therapy

- **External beam radiation therapy** – standard external beam radiation therapy for CaP consists of between 75.6 and 81.0 Gy of radiation separated into 1.8- to 2- Gy doses (or "fractions") given daily for between 7 and 9 weeks. Recently, relatively shorter treatment schedules delivering more radiation per treatment over shorter time periods have been proposed in an effort to cut down rising health care costs and improve patient convenience. However, significant uncertainty still remains regarding outcomes from this type of more condensed treatment, known as "hypofractionated" radiation (Aneja et al. 2012).
- **Intensity modulated radiation therapy** – this regime achieves higher prostate radiation dose and less radiation to surrounding tissue because it offers more precise control over the radiation field (Biagioli et al. 2010).
- **Proton beam therapy** – promising variant of radiotherapy, since unlike x-rays, which release

energy both before and after they hit their target, proton beams deposit almost all their radiation dose at the end of the particle's path in tissue thus causing lesser damage to the healthy tissues (Heidenreich et al. 2011).

- **Brachytherapy** – precise placement of short-range radiation-sources directly at the site of the cancerous tumor under transrectal ultrasound guidance. A key feature of this technique is that the irradiation only affects a very localized area around the radiation sources. Brachytherapy to treat CaP can be given either as permanent low-dose-rate (LDR) seed implantation or as temporary high-dose-rate (HDR) brachytherapy (Yoshioka et al. 2009).

1.5.3.2. Radioresistance of prostate cancer

Various forms of radiation therapy (RT) are one of the most popular treatment options for clinically localized CaP. In combination with radical prostatectomy, it is the most successful therapeutic modality significantly improving metastasis free survival and overall survival, where the median of 15-year survival is around 47% (Heidenreich et al. 2011, Mottet et al. 2011). However, the rest of patients develop metastatic form of cancer that is incurable due to the resistance of CaP cells to androgen ablation, RT and current chemotherapeutics. There are many factors implicated in RT failure and current effort is to define as many of them as possible to focus on those which could be targeted efficiently.

Part of the radioresistance effect can be explained by evasion from the irradiated area. This concerns the cells located at the edge of the irradiated field, as well as the cells that manage to escape by perineural or lymphatic invasion (Bonkhoff 2012). However, even the properly irradiated cells can develop radioresistance by activating certain signalling pathways.

Androgen receptor signaling

In CaP many survival pathways are closely bound to AR signalling and there are many ways how cells put this particular pathway out of balance. The most significant are: upregulation of AR expression, increased intratumoral synthesis of androgens, AR gene mutations associated with altered ligand specificity (leading to AR activation by nonandrogenic steroid molecules or even to a sustained activation with no need for ligand binding) and AR pathway activation downstream the AR (Bonkhoff 2012, Locke et al. 2008, Attard et al. 2006, Amaral et al. 2012).

Cell cycle regulators

Apart from the AR signalling, many other pathways are implicated in cell proliferation and their imbalance can contribute to RT failure. Not surprisingly, pathways concerning some of the key regulators of the cell cycle can be found among them. Loss or downregulation of cell cycle repressors may lead to aberrant proliferation and higher risk of RT failure, which has been shown for PTEN (Heinlein and Chang 2004, Rosser et al. 2009), p27kip1 (Cheng et al. 2000), p16INK4A (Roach et al 2009) or Wee1 kinase (Kiviharju-af Hällström et al. 2007). Conversely, positive regulators of cell cycle, such as protein kinase A type 1 are often highly expressed in radioresistant and aberrantly proliferative CaP cells (Hensley et al. 2011, Pollack et al. 2009).

DNA damage response

Correlation between expression level of particular components of DNA damage pathways and response to ionizing radiation has been reported repeatedly (Collis et al. 2003, Schaue and McBride 2005, Serafin et al. 2007, Lu et al. 2008, Sanli et al. 2010, Shaheen et al. 2011, Rashid et al. 2011, Barreto-Andrade et al. 2011, Mahajan et al. 2012, Chiba et al. 2012, Sugrue et al. 2013, Wang et al. 2012). Targeting some of the key proteins, such as ATM, ATR, Chk1, Chk2, DNA-PK, XRCC4, GADD45A, PARP, and DNA Ligase IV, has resulted in increased radiosensitivity (Collis et al. 2003, Schaue and McBride 2005, Lu et al. 2008, Sanli et al. 2010, Shaheen et al. 2011, Barreto-Andrade et al. 2011, Wang et al. 2012).

Resistance to apoptosis

Even though terminal growth arrest rather than apoptosis seems to be the major endpoint in CaP following RT (Bromfield et al. 2003), apoptotic pathways are still important determinants of radioresponse. The well-known anti-apoptotic proteins favouring radioresistance are Bcl-2 (Rosser et al. 2003, Quinn et al. 2005) and Mdm2 (Khor et al. 2009, Stoyanova et al. 2007), whereas p53, mediator of G1 cell cycle arrest and apoptosis following DNA damage, makes the cells more accessible to radiation treatment (Quinn et al. 2005, Roach et al. 2009).

Growth factor receptors

CaP cells can maintain proliferation and survival through activation of growth factor receptors, including epidermal growth factor receptor family members, vascular endothelial growth factor receptor (VEGFR), insulin-like growth factor receptor, keratinocyte growth factor receptor, transforming growth factor receptor *β*, and interleukin-6 receptor. These growth factors and their receptors phosphorylate the AR via mitogen-activated protein kinases and PI3K/Akt/mTOR signalling (Culig 2004, Zhu and Kyprianou 2008). Besides, there are various other mechanisms by which growth

factor receptors mediate failure of RT. Epidermal growth factor receptor family members, for example, regulate hypoxia-inducible factor 1α (HIF-1α) and VEGF expression, thus promoting angiogenesis (Karar and Maity 2009).

Hypoxia

Hypoxia and tissue acidification are other determinants of RT failure. In hypoxic milieu, HIF-1 and VEGF are upregulated, promoting angiogenesis. Furthermore, NF-*κ*B and Stat3 pathways are activated, while both of the factors have been repeatedly associated with tumor metastasis and NF-*κ*B also with cell survival, proliferation and castration resistance (Ross et al. 2004, Jin et al. 2008, Abdulghani et al. 2008).

Cancer stem cell phenomenon

Cancer stem cells are characterized as rare and undifferentiated cells that continually resupply tumor cells under androgen deprivation therapy, RT and other cytotoxic conditions, and may be responsible for therapy failure. They are considered multidrug-resistant, with no AR on their surface (Collins et al. 2005).

Other mechanisms

From other mechanisms which are supposed to be implicated in CaP radioresistance, we can mention differentiation into neuroendocrine cells (Bonkhoff 2012), expression of DOC-2/DAB2 interactive protein (Kong et al. 2010), cyclooxygenase-2, heat shock proteins (Bonkhoff 2012), clusterin (Zellweger et al. 2002) or superoxide dismutases (Niciforovic et al. 2008). Conversely, expression of other proteins such as FOXP3 sensitizes cells to radiation (Li et al. 2013).

1.6. Previous achievements and project description

1.6.1. Preliminary results

In our preliminary experiments related to this project, we exposed various metastatic CaP cell lines (DU145, PC-3, LNCaP, and 22RV1) to irradiation regimes used in current radiotherapy of CaP patients. We followed phenotypic features occurring not only during the radiation treatment but also in surviving “radioresistant” populations.

Main findings of our preliminary experiments can be summarized as follows:

- There are at least three phenotypically distinct populations surviving 70 Gy of fractionated radiation derived from metastatic CaP cell lines (Fig. I):
    - adherent cells undergoing phenotype resembling cellular senescence
    - cells losing adhesion during radiation treatment and resistant to anoikis – non-adherent "floating" cells
    - adherent cells stemming from floating cells after their readhesion – "readherent" cells.
- Radiation treatment induces activation of cell cycle inhibitors $p21^{waf1/cip1}$ (p21) and $p27^{kip1}$ (p27) together with persistent levels of cell cycle activators (cyclin D1).
- EMT-specific transcription factors Snail1, Twist1 and Slug are elevated in DU145 floating cells, whereas another EMT transcription factor ZEB2 is elevated in PC-3 floating cells.
- Notch signaling pathway and Erk signaling (invovlved in Snail regulation) are induced by radiation in both DU145 and PC-3 floating cells.
- Knock-down of Snail1 decreases significantly absolute numbers of non-adherent cells in irradiated DU145 sample almost to the level of non-irradiated control
- Readherent cells posses more pronounced epithelial features and decreased migration in comparison to parental cells.
- Floating cell fraction has elevated levels of antiapoptotic proteins - possible basis of the resistance to anoikis.

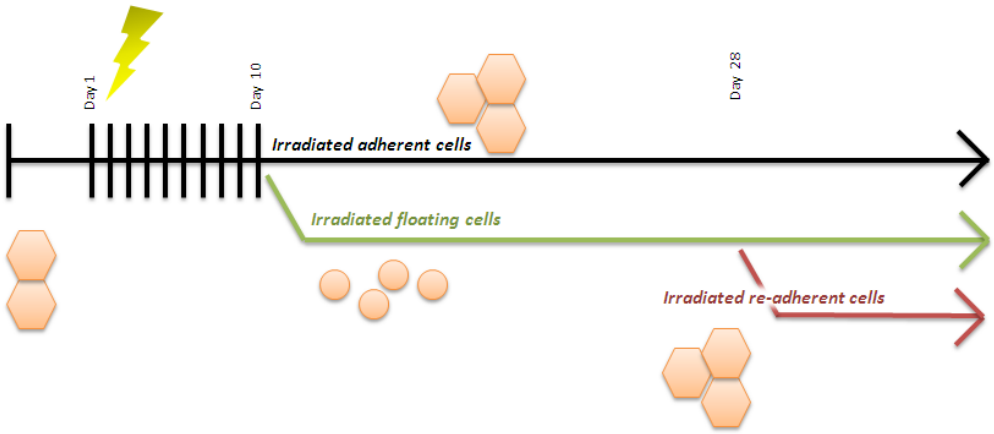

Figure I: Three populations of cells arising from radiation treatment. (According to L. Kyjacová)

Based on these results we propose that cellular plasticity (i.e. dynamic transitions between epithelial, mesenchymal and stem cell phenotype) is induced in cancer cells with mitigated tumor suppressor function directly by genotoxic stress-activated DNA damage response. Our hypothesis is supported by previous findings in other tissues. For example, it has been published recently, that ionizing radiation induces reprogramming of breast cancer cells to a stem cell phenotype (Lagadec et al. 2012) or causes long-term tumor cell dissemination and metastasis by facilitating EMT in hepatocellular carcinoma (Li et al. 2011). In CaP ionizing radiation has been reported to induce neuroendocrine differentiation (Deng et al. 2011), one of the putative radioresistance mechanisms (see chapter 4.3.2.8).

1.6.2. The aims of the project

- We have noticed that radiation induces cells detachment, however, we have not determined precisely, how many cells detach after irradiation and how many live cells this floating fraction contains. We want to measure these parametres in comparision with non-irradiated control population.
- Elevated levels of several EMT markers have been observed in irradiated floating fractions. Therefore, we are interested, whether these and other EMT markers are elevated also in adherent fractions of irradiated cells. Immunofluorescent labeling will be used to accomplish this task, to monitor not only changes in protein levels but also changes in protein localization.
- EMT and radioresistance are tightly bound to stemness. Thus, we would like to measure levels of selected stem cell markers in control and irradiated foating fractions. For this measurement we will use flow cytometry, a method, which is snsitive enough to detect cells with low abundancy, which stem cells are.
- Irradiated floating cells have elevated levels of cell cycle inhibitors. We are thus interested, what are the cell cycle profiles of adherent and floating cells in control and irradiated population. To asses the cell cycle profiles, propidium iodide-based cell cycle analysis by flow cytometry will be performed.
- γ-radiation has repeatedly been reported to slow down or inhibit cell proliferation. Therefore, we would like to discribe the impact of γ-radiation on proliferation rate of adherent and floating fractions of irradiated cells. Dyeing cells with Cell Proliferation Dye eFluor 670 (eBioscience) and measurment of the dye intensity by flow cytometry will be used in this task.

- Irradiated floating cells remain in a suspension for a few days, after that they are able to readhere and set up readherent population. We would like to know, how the proliferation rates of individual fractions change during this process. The technique based on Cell Proliferation Dye eFluor 670 (eBioscience) will be used here again.
- Readherent population of cells has been only poorly characterized. Thus, we want to estimate the levels of selected epithelial, esenchymal and stem cell markers in these cells by immunofluorescence microscopy and flow cytometry.

2. Materials and methods

2.1. Introduction to the methods

2.1.1. Ionizing radiation

Radiation is the energy carried by either electromagnetic waves or moving particles and according to its effect on atoms and molecules it can be divided into ionizing and non-ionizing type. Ionizing radiation (IR) is composed of particles that individually carry enough kinetic energy to liberate an electron from an atom or molecule, thus ionizing it. It includes cosmic rays, neutrons, alpha particles, beta particles, gamma rays, X-rays, and in general any charged particle moving at relativistic speeds.

The international (SI) unit for absorbed dose is the gray (Gy), which is defined as 1 joule of energy deposited in 1 kilogram of mass. The old unit of measure for this is the rad, which stands for "radiation absorbed dose." - 1 Gy = 100 rad. The effect of radiation further depends on the intensity of ionisation in living cells caused by different type of radiations. Neutron, proton and alpha particle can cause 5-20 times more harm than the same amount of the absorbed dose of beta or gamma radiation.

The unit of equivalent dose is the sievert (Sv), SI unit representing the biological effects of ionizing radiation. Use of the sievert implies, that appropriate regulatory weighting factors have been applied to the original measurement. For example, an absorbed dose of 1 mGy of alpha radiation gives an equivalent dose of 20 mSv because alpha particle has a radiation weighting factor of 20. Each member of the world population is exposed, on average, to 2.4 mS of ionizing radiation per year from natural sources (http://www.icrp.org/publication.asp?id=ICRP%20Publication%20103).

Radiation-induced ionization may act directly on the cellular component molecules or indirectly on water molecules, causing water-derived radicals. Radicals react with nearby molecules, resulting in breakage of chemical bonds or oxidation of the affected molecules (http://www.rerf.jp/radefx/basickno_e/radcell.htm). In cells, the major effect is damage of molecules that regulate vital cell processes (e.g. DNA, RNA, proteins). In terms of DNA, there are three possible scenarios following radiation-caused damage: either the cell is able to repair its DNA and to continue living normally, or it is not able to repair the DNA perfectly, which leads to DNA mutations (the principle of radiation-induced carcinogenesis and other health problems), or the DNA damage or consequent DNA rearrangement is so extensive that it is not compatible with living and cell death occurs. This last scenario is used in radiotherapy, when high but tolerable doses of ionizing

radiation are targeted at tumor tissue causing serious DNA damage, leading ideally to cell death and tumor disappearance.

2.1.2. Immunofluorescence

Immunofluorescence (IF) is a common laboratory technique used in almost all aspects of cell biology. Applications include the evaluation of cells in suspension, cultured cells, tissue, beads and microarrays for the detection of specific proteins. Immunfluorescent techniques can be used on both fresh and fixed samples. In antibody-based immunofluorescent techniques, antibodies are chemically conjugated to fluorescent dyes. These labeled antibodies bind (directly or indirectly) to the antigen of interest which allows for antigen detection through fluorescence techniques. The fluorescence can then be quantified using a flow cytometer, array scanner or automated imaging instrument, or visualized using fluorescence or confocal microscopy.

Immunofluorescent labeling can be either direct or indirect. In direct immunofluorescence, the antibody against the molecule of interest is chemically conjugated to a fluorescent dye. In indirect immunofluorescence, the specific antibody (so called primary antibody) is unlabeled, and a second anti-immunoglobulin antibody directed toward the constant portion of the first antibody (called the secondary antibody) is tagged with the fluorescent dye (http://www.dako.com/08002_03aug09_ihc_guidebook_5th_edition_chapter_10.pdf).

2.1.3. Flow cytometry

Flow cytometry is the measurement of cells in a flow system, which delivers the single cells to a point of measurement. In theory, there are many types of measurements that could be made, but in practice, the light is focused at the point of measurement and the scattered light and fluorescence are recorded. Typically, light scatter at two different angles and fluorescence of different wavelenghts (from one to six fluorescence channels) are measured. Although cells are usually analysed, other particles, such as nuclei, chromosomes or small beads, can also be studied.

Some organisms, such as marine algae, are inherently fluorescent, but in general, the fluorescence arises from different labels. Some fluorescent chemicals possess the ability to label cell components (such as DNA) directly; others are attached to antibodies against a wide variety of cellular proteins.

The value of the technique lies in the ability to make measurements on large numbers of single cells within a short period of time (tens of seconds to minutes). The heterogeneity

of populations can be revealed and different subsets of cells identified and quantified. Selected cell populations can also be physically sorted for further study. The major disadvantage of flow cytometry is that it requires a suspension of single cells or other particles, with minimum clumps and debris. This means that the tissue architecture and any information about the spatial relationship between different cells are lost when single cells or nuclei are prepared.

Data are usually shown either as single parameter histograms or as two parameter correlated plots, often called cytograms. A cytogram may be presented as a dot plot, a density or a contour plot. In a dot plot, each cell recorded is shown as a single dot. This is the form in which data are shown during data acquisition (http://flowbook.denovosoftware.com/Flow_Book/Chapter_1%3a_ Introduction).

2.1.4. Cell cycle analysis by flow cytometry

One of the earliest applications of flow cytometry was the measurement of DNA content in cells; the first rapid identification of phases of the cell cycle other than mitosis. This analysis is based on the ability to stain the cellular DNA in a stoichiometric manner (the amount of stain is directly proportional to the amount of DNA within the cell). A variety of dyes are available to serve this function, all of which have high binding affinities for DNA. The location to which these dyes bind on the DNA molecule varies with the type of dye used.

The two most common categories of DNA binding dyes in use today are the blue-excited dye propidium iodide (or occasionally the related dye ethidium bromide) and the UV-excited dyes diamidino-phenylindole (DAPI) and Hoechst dyes 33342 and 33258. Propidium idode is an intercalating dye which binds to DNA and double stranded RNA (and is thus almost always used in conjunction with RNAse to remove RNA), while DAPI and Hoechst dyes bind to the minor groove of the DNA helix and have essentially no binding to RNA. Hoechst 33342 has the distinction of being the only dye presently available which allows satisfactory DNA staining of viable cells. The other dyes require permeabilization of the cell membrane before staining, most often by detergent or hypotonic treatment or by solvent (e.g. ethanol) fixation.

Whichever DNA-binding fluorescent dye is used, a characteristic pattern is seen that reflects the cell cycle phases that make up the mixed cell population.

When diploid cells, which have been stained with a dye that stoichiometrically binds to DNA, are analyzed by flow cytometry, a “narrow” distribution of fluorescent intensities is obtained. This is displayed as a histogram of fluorescence intensity (X-axis) vs. number of cells with each observed intensity. Since all G1 cells have the same DNA content, exactly the same

fluorescence should in theory be detected from every G1 cell, and only a single channel in our histogram would be filled. In practice, however, there are a variety of sources of instrumental error in cytometers, in addition to some biological variability in DNA dye binding. Consequently, the measured fluorescence from G1 cells is a normally distributed Gaussian peak.

Similarly, G2 and mitotic cells, described as having twice the normal G1 DNA content, produce a Gaussian peak in the DNA content histogram with a mean position approximately twice that of the G1 peak.

In a theoretically perfect flow cytometer, S phase cells would be observed in the histogram starting just above the position occupied by all the G1 cells, and some of the S phase cells would be found in each channel extending up to just below the position of all the G2 cells. Unfortunately, the same factors, which broaden the G1 and G2 peaks also, broaden the S phase distribution, which results in early S phase cells overlapping with G1 cells, and late S phase cells overlapping with G2 cells (http://www.phnxflow.com/Introduction%20to%20Cell%20Cycle%20Analysis.pdf).

2.1.5. Cell proliferation dye

Cell Proliferation Dye eFluor® 670 is a red fluorescent dye that can be used to monitor individual cell divisions. This fluorescent dye binds to any cellular protein containing primary amines, and as cells divide, the dye is distributed equally between daughter cells that can be measured as successive halving of the fluorescence intensity of the dye (http://www.ebioscience.com/cell-proliferation-dye-efluor-670.htm).

2.2. Materials and methods for this project

2.2.1. Cell line and culture

The DU145 cell line was purchased from ATCC™ and cultured in DMEM (Gibco®) supplemented with 10% heat inactivated fetal bovine serum (Gibco®) and 0.25% penicillin/streptomycin. Cells were cultured in 15cm dishes with 35 mL of complete DMEM, at 37°C in 5% CO_2.

2.2.2. Irradiation of cells and obtaining fractions

The cells were irradiated ten times over a time course of 10 days with a dose of 2 Gy using X-ray generator (Pantak, Berkshire, United Kingdom). On the first day of irradiation cells were 90% confluent. The analysis was performed two hours after individual irradiation time points. Cells were not passaged for the whole ten days, but medium was changed after five days.

During irradiation, some of the cells detached from surface and started to float in medium. The same phenomenon occurred in control dishes, even though they were not irradiated. The detached cells were named "*floating* fraction" and analysed separately from the "*adherent* fraction". During medium change, the floating fraction was removed, centrifuged, resuspended in a fresh DMEM and put back to the parental adherent population.

To obtain "*readherent* fraction", floating cells after 10 day irradiation treatment were harvested, spun down, resuspended in 35 mL of fresh medium and replated on a new 15cm dish. The cells were cultured for 28 days without replating; medium was changed every seven days. After 28 days several colonies of readherent cells appeared on the dish.

2.2.3. Immunofluorescence

50,000 cells were seeded into each chamber of an eight-chamber BD Falcon™ CultureSlide and cultured for three days in 0.5 mL of DMEM supplemented with 10% of heat inactivated FBS and 0.25% penicillin/streptomycin. Slides were irradiated as described above.

For analysis, cells in each chamber were washed once with 500 µL of 1 x PBS, fixed for 10 min with 500 µL of 1:1 methanol/acetone in 4°C, washed in 500 µL of 1 x PBS again, blocked for 20 min in 500 µL of 1 x PBS with 2% milk powder and stained with 100 µL of 1 x PBS containing diluted primary antibodies (see the Table 2) at 4°C in dark. The next day cells were washed 3 x 5 min in 500 µL of 1 x PBS, stained with 100 µL of 1 x PBS with diluted secondary antibodies for 45 min in dark, washed 3x 5 min in 500 µL of 1 x PBS again and counterstained with VECTASHIELD® HardSet™ Mounting Medium with DAPI (Vector Laboratories).

Finally, the glass slides were sealed with nail polish and examined by fluorescence microscopy (Axio Imager.A2, ZEISS, Germany).

2.2.4. FACS analysis – mesenchymal and stem cell markers

Floating cells were harvested from the dishes together with medium. Adherent fraction was washed with 1 x DPBS to get rid of the loosely attached cells. The PBS from the washing step was added to the tube with the floating fraction and the tubes were kept on ice.

Adherent fraction was incubated with 6 mL of the calcium chelating agent Versene (Gibco®), until the cells detached (approximately 1 h). Then 4 mL of DMEM were added to the dish and this suspension was transferred into a separate tube. Finally, each dish was washed with 5 mL of DMEM and these 5 mL were added to the tube containing adherent fraction. The tubes were also kept on ice.

Cells were counted and spun down in a cooled centrifuge (4°C), 5 min at 300 x g.

2.5 x 10^5 cells of each cell fraction were resuspended in 100 µL of 2% FBS in 1 x PBS and stained with antibodies (see the Table 2) and Hoechst 33258 pentahydrate (INVITROGEN, final concentration 10 µg/mL) for 45 min at 4°C in the dark. After washing with 3 ml of 2% FBS in 1 x PBS, the cells were resuspended in 400 µL of 2% FBS in 1 x PBS and analyzed using a FACSVerse (BD Bioscience) flow cytometer.

2.2.5. FACS analysis – cell proliferation

2.2.5.1. Dyeing and culturing of floating cells after irradiation treatment

Floating fractions of ten times irradiated cells and respective control cells were obtained as described above. Cells were dyed with Cell Proliferation Dye eFluor® 670 (eBioscience) according to enclosed protocol and fluorescence intensity was measured immediately after dyeing. Dyed cells were seeded onto 2 x 4 10cm dishes – 4 dishes for controls and 4 dishes for irradiated cells. At four time points (6 days, 12 days, 20 days and 28 days after dyeing) always one control and one experimental dish was analyzed by flow cytometry. From certain time points (different for control and irradiated cells) some cells adhered back to the dish surface. These cells were analyzed separately from the floating fraction as so called readherent fraction.

2.2.5.2. Dyeing of adherent cells before irradiation treatment and their subsequent irradiation

Normally cultured DU145 cells were dyed Cell Proliferation Dye eFluor® 670 (eBioscience) according to enclosed protocol and fluorescence intensity was measured immediately after dyeing.

Dyed cells were seeded onto four 15cm dishes – 2 dishes for control cells and 2 dishes for irradiated cells. The latter two dishes were irradiated every day with 2 Gy of ionizing radiation for the period of five and ten days, respectively. The 5th and 10th day of irradiation, approximately two hours after receiving the last dose, always one control dish and one irradiated dish were analyzed by flow cytometry.

2.2.5.3. Preparation of the samples for FACS analysis

Floating cells were harvested from the dishes together with medium. Adherent fraction (if present) was washed with 1 x DPBS to get rid of the loosely attached cells. The cells from the washing step was added to the tube with the floating fraction, spun down and resuspended in 1mL of the calcium chelating agent Versene (Gibco®).

Adherent fraction was incubated with 3 mL (for 10cm dish) or 6 mL (for 15cm dish) of Versene, until the cells detached from the dish (more than 1 h). Then 2 mL (for 10cm dish) or 4 mL (for 15cm dish) of DMEM were added to the dish and this suspension was transferred into a separate tube. Finally, each dish was washed with 3 mL of DMEM (for 10cm dish) or 5 mL of DMEM (for 15cm dish) and these were added to the tube containing adherent fraction. The tubes were kept on ice.

Cells from both adherent and floating fraction were counted and spun down in a cooled centrifuge (4°C), 5 min at 300 x g. 2.5 x 10^5 cells of each cell fraction were washed in 3 mL of 1 x PBS, resuspended in 400 µL of 1 x PBS and analyzed using a FACSVerse (BD Bioscience) cytometer.

2.2.6. FACS analysis – cell cycle profile

2.2.6.1. Cell fixation and viability dyeing

Cells were irradiated as described above (see “Irradiation of cells and obtaining fractions”). After receiving the last dose, floating cells were harvested from the dishes together with culture medium. Adherent fraction was washed with 1 x DPBS to get rid of the loosely attached cells. The PBS from the washing step was added to the tube with the floating fraction and the tubes were kept on ice.

Adherent fraction was incubated with 6 mL of the calcium chelating agent Versene, until the cells detached (approximately 1 h). Then 4 mL of DMEM were added to the dish and this suspension was transferred into a separate tube. Finally, each dish was washed twice with 5 mL of DMEM and these 5 mL were added to the tube containing adherent fraction. The tubes were also

kept on ice.

Prior to fixation, cells were stained by Fixable Viability Dye eFluor® 780 (eBioscience) according to enclosed protocol.

After that, cells were spun down in a cooled centrifuge (4°C), 5 min at 300 x g and the pellets were resuspended in 300 µL of 1 x PBS. 700 µL of 96% ethanol were added into each tube and the tubes were kept in a cold room.

2.2.6.2. DNA labelling with propidium iodide and cell cycle profile analysis

The fixed cells were counted, spun down in a cooled centrifuge (4°C), 5 min at 300 x g and the pellets were washed with 2 mL of 1 x PBS. Then 2.5 x 10^5 cells of each cell fraction were resuspended in 100 µL of 2% FBS in 1 x PBS and stained with 5 µL of propidium iodide with RNAse for 15 min at 4°C in the dark. After washing with 2 ml of 2% FBS in 1 x PBS, the cells were resuspended in 400 µL of 2% FBS in 1 x PBS and analyzed using a FACSVerse (BD Bioscience) flow cytometer.

Antibody	Species	Type	Vendor	Order number	Dilution
Immunofluorescence					
β-catenin	rabbit	mono	BD Transduction Laboratories	610153	1:200
E-Cadherin (24E10)	rabbit	mono	Cell Signalling	3195	1:100
phospho-Histone H2A.X (Ser139)	mouse	mono	Milliphore	05-636	1:400
Anti-gamma H2A.X (phospho S139)	rabbit	poly	Abcam	ab2893	1:400
Snail1	rabbit	poly	Abcam	ab17732-100	1:100
Slug (Snail2)	rabbit	poly	Abcam	ab27568	1:100
FITC Anti- E-Cadherin	mouse	mono	BD Transduction labs	612130	1:400
vimentin	goat	poly	Sigma	V4630	1:100
Twist	rabbit	poly	Abcam	ab50581	1:200
Flow cytometry					
PE Mouse Anti-Human CD44	mouse	mono	BD Pharmingen	555479	5 µl per 250 000 cells
PerCP/Cy5.5 anti-human/mouse CD49f Antibody	mouse	mono	Bio Legend	313617	2 µl per 250 000 cells
Alexa Fluor® 488 anti-human CD324 (E-Cadherin) Antibody	mouse	mono	Bio Legend	324110	1,5 µl per 250 000 cells
CD 133/1 (AC 133) - APC	mouse	mono	MACS Mileny Biotec	130-090-826	5 µl per 250 000 cells

Table 2: List of antibodies

3. Results

3.1. Expression of selected epithelial, mesenchymal and stem cell antigens in control cells

In order to compare the expression of epithelial, mesenchymal and stem cell markers in prostate cancer before and after radiation, we examined two cell lines, DU145 and PC-3.

Non-irradiated cells of both cell lines were stained by immunofluorescence with antibodies against vimentin, fibronectin, N-cadherin (mesenchymal markers), Twist1, Snail (Snail1) and Slug (Snail2; EMT inducers), E-cadherin (epithelial marker) and β-catenin (Lee et al. 2006). β-catenin has a dual role in EMT; it enhances cell–cell adhesion when bound to E-cadherin complexes in adherens junctions and also functions as a transcriptional coactivator upon entry into the nucleus (Lee et al. 2006). Therefore, it can be used both as epithelial and mesenchymal marker, depending on its localization.

We found that PC-3 cells have overall much higher level of mesenchymal markers fibronectin and Twist1 (Fig. 1B, C). Furthermore we noticed that there are two distinct populations of both DU145 and PC-3 cells. One population has high levels of membrane E-cadherin and β-catenin, showing that these cells are more epithelial, whereas the other population has very low levels of these proteins and can be thus considered more mesenchymal (Fig. 1A).

We confirmed these results by flow cytometry, where we wanted to examine DU145 and PC-3 cell lines with respect to expression of four antigens:

- E-cadherin, a well established epithelial marker
- CD44, the basal cell marker, mesenchymal marker and putative prostate stem cell marker in combination with other antigens (Chen et al. 2012, Colombel et al. 2012, Goldstein et al. 2010, Guo et al. 2012, Liu 2000, Tu and Lin 2012, Yu et al. 2012)
- CD49f (integrin α6), basal cell marker and putative prostate stem cell marker (Colombel et al. 2012, Goldstein et al. 2010, Guo et al. 2012, Liu et al. 2000, Yamamoto et al. 2012)
- CD133, putative prostate stem cell marker (Chen et al. 2012, Colombel et al. 2012, Guo et al. 2012, Tu and Lin 2012, Yu et al. 2012).

Regarding CD44, CD49f and CD133, there was only one population of cells in both cell lines, ranging from low to high fluorescence intensity. On the contrary, while examining E-cadherin levels, we detected two populations of cells within each cell line, one of them being E-cadherin low and the other E-cadherin high. In DU145 line, there were also some cells of intermediate phenotype,

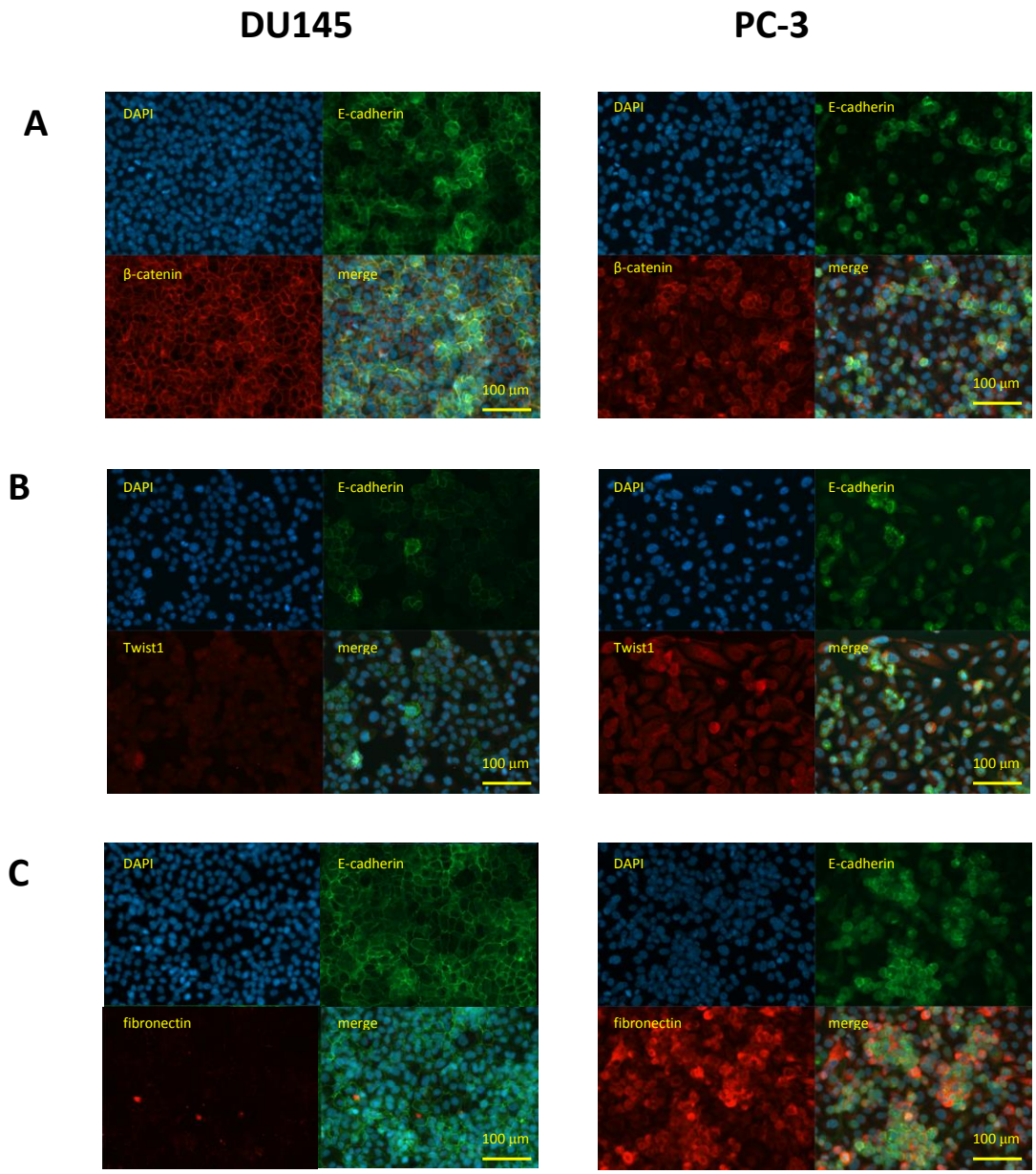

Figure 1: Expression of epithelial and mesenchymal markers in DU145 and PC-3 prostate cancer cell lines shown by immunofluorescence. A) DAPI (blue), E-cadherin (green) and β-catenin (red). **B)** DAPI (blue), E-cadherin (green) and Twist1 (red). **C)** DAPI (blue), E-cadherin (green) and fibronectin (red).

connecting these two populations together and forming continuous transition between them. In PC-3 cells, on the contrary, the two populations were clearly distinct and only few cells of intermmediate phenotype were observed (Fig. 2A, B).

Considering the results of these two experiments, we figured that it would be difficult to draw any conclusions from the experiments with PC-3 cells, because we would not be able to distinguish, whether radiation induced changes in the cell phenotype or whether it only selected

for one of the populations. DU145 cells, on the other hand, expressed all the examined markers more uniformly, so we decided to use these cells for further experiments.

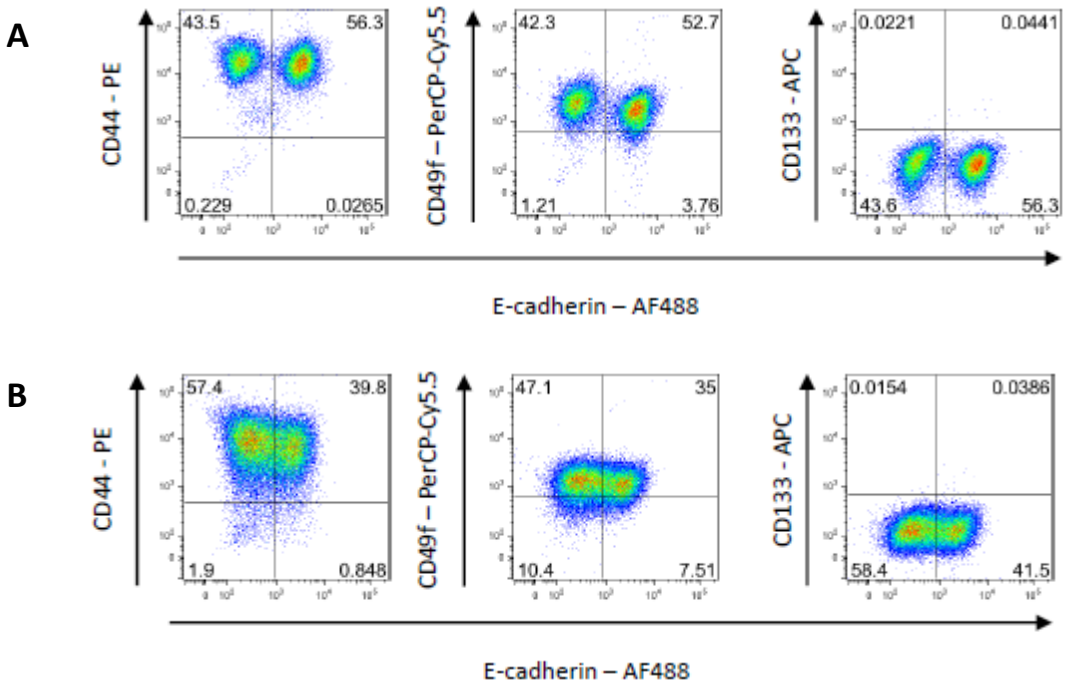

Figure 2: Expression of E-cadherin, CD44, CD49f and CD133 estimated by flow cytometry. A) PC-3 cell line **B)** DU145 cell line

3.2. Cell survival and cell floating after irradiation

Survival rate was calculated after 5 and 10 doses of irradiation using flow cytometry. As expected, after five and ten doses of radiation, there were more live cells in control fractions than in irradiated ones. Similarly, we could find more live cells in adherent fractions than in floating fractions. The percentage of live cells in all four fractions (control adherent, control floating, irradiated adherent and irradiated floating) was always higher after five doses than after ten doses of irradiation (Fig. 3A, 3B). The only exception was control floating fraction, where there were more live cells after ten days of irradiation than after five days. It is likely, that after ten days the cells were already over-confluent and even the living cells without serious damage were released into medium simply because there was no more space on the dish.

Then we counted how many cells start floating after 5 and 10 days of everyday irradiation. The percentage of floating cells was always higher in irradiated cells than in controls. After ten doses of irradiation, floating cells comprised as much as 70% of the whole population (Fig. 4).

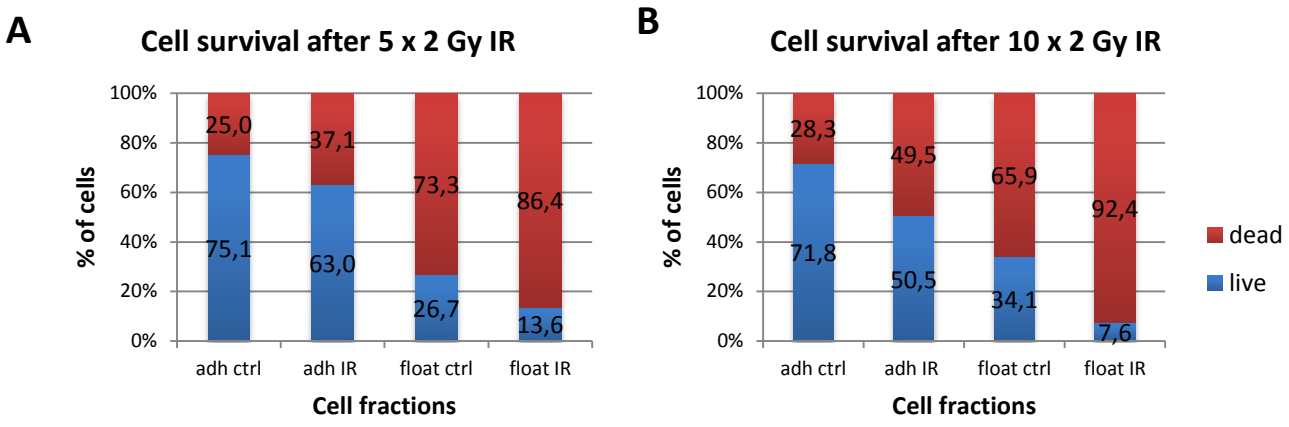

Figure 3: Cell survival after ionizing radiation. DU145 cells after **A)** 5 doses **B)** 10 doses of ionizing radiation

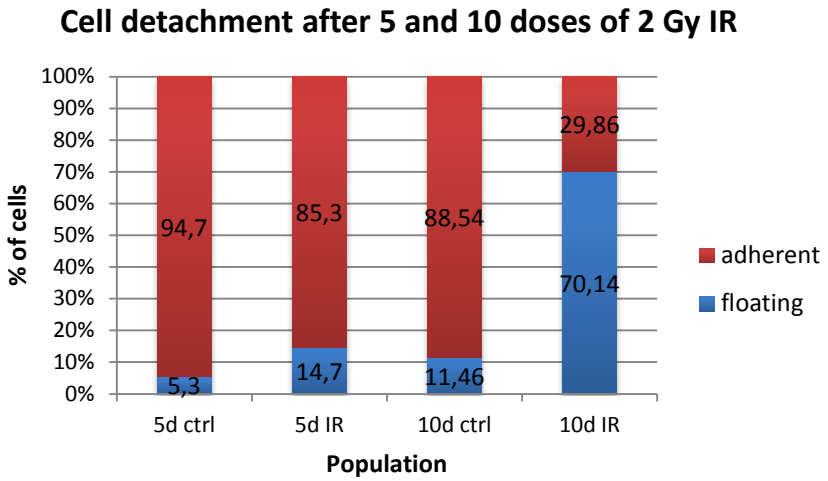

Figure 4: Cell detachment after ionizing radiation. DU145 cells after 5 and 10 doses of ionizing radiation.

Combined graph, depicting the structure of the whole populations after five and ten doses of irradiation in both irradiated and control cells is shown in Fig. 5.

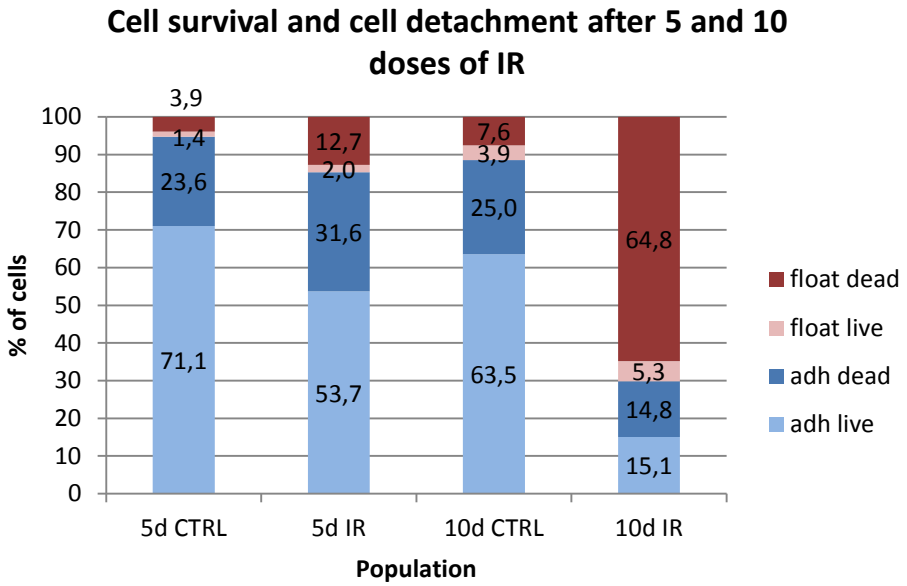

Figure 5: Cell survival and cell detachment after ionizing radiation. DU145 cells after 5 and 10 doses of ionizing radiation. Cell survival estimated by flow cytometry.

3.3. Expression of selected mesenchymal markers after irradiation

We seeded the cells of DU145 cell line onto eight-chamber culture slides as described in Materials and Methods. Two slides were irradiated every day with 2 Gy for 5 days and 10 days, respectively. Two other slides were used as non-passaged controls. After fixation, we stained adherent cells with the following antibodies: vimentin, fibronectin, Snail1, Slug (Snail2), Twist1 and N-cadherin (mesenchymal markers), E-cadherin (epithelial marker), histone H2A.X phosphorylated on serine 139 (marker of DNA damage, Rogakou et al., 1998) and β-catenin.

As expected, there was an increase in the DNA damage marker, γH2A.X both 5 and 10 days after irradiation showing efficient DNA damage. In both control samples only a few cells formed a low number of γH2A.X nuclear foci, whereas in five and ten times irradiated cells the number of foci-forming cells was much higher, as well as the number of foci per nucleus (Fig. 6A). Apart from that, we detected a slight increase in an EMT inducer, Snail1 (Fig. 6B) in five and ten times irradiated cells, compared to relevant controls. E-cadherin levels were not substantially changed in irradiated adherent cells. We did not notice considerable changes in the level or localization of any of the remaining proteins (data not shown).

Taken together it seems that unlike in irradiated floating cells, ionizing radiation has only minor influence on expression of epithelial and mesenchymal markers in adherent fraction of DU145 prostate cancer cell line.

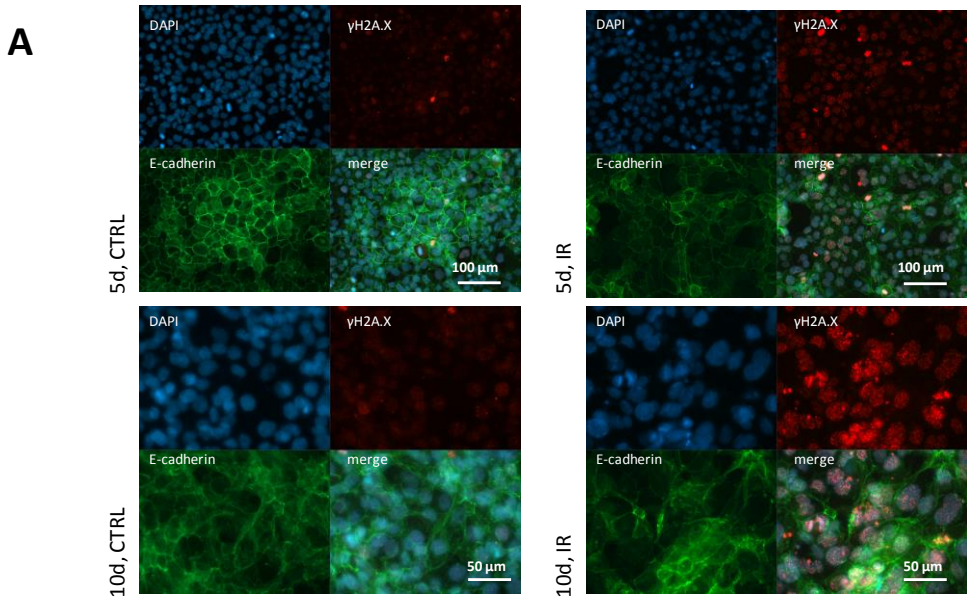

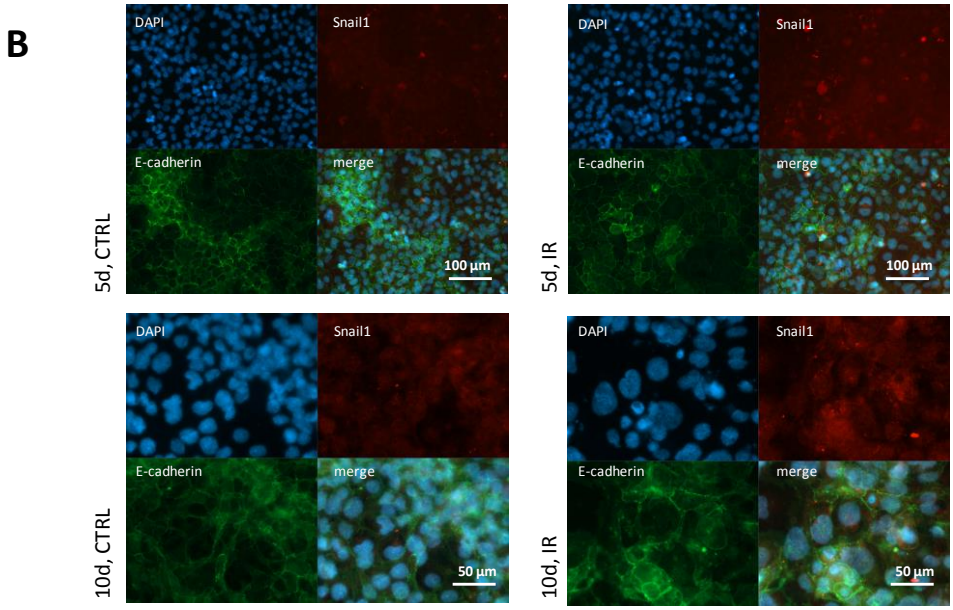

Figure 6: Expression of selected markers in DU145 cell line after irradiation. Expression of E-cadherin, γH2A.X and Snail1 in control, five times irradiated and ten times irradiated cells. **A)** γH2A.X, **B)** Snail1, **A) B)** E-cadherin

3.4. Expression of selected mesenchymal and stem cell markers decreases in floating cell fraction, but ionizing radiation seems to counteract this process

Using flow cytometry we examined the presence and levels of several antigens, epithelial, mesenchymal and stem cell markers, namely: E-cadherin (a well established epithelial marker), CD 44 (the mesenchymal marker and putative prostate stem cell marker), CD49f (integrin subunit α6; putative prostate stem cell marker) and CD133 (putative prostate stem cell marker).

Cells were irradiated 10 times with the dose of 2 Gy and subsequent analysis was performed the 5th and 10th day of irradiation, two hours after receiving the last dose. As a control we used cells, which were seeded the same day at the same density, but were not irradiated and replated. Two fractions were monitored in irradiated and control sample: adherent and floating.

As we expected, most of the cells within the population of irradiated and control adherent cells were E-cadherin positive. Notably, the populations of irradiated and control floating cells were E-cadherin negative.

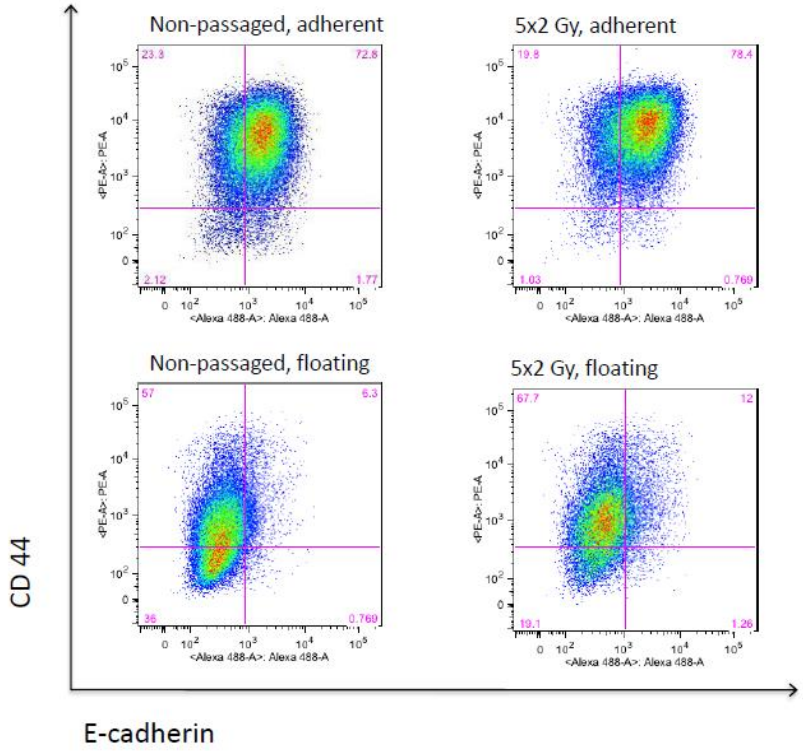

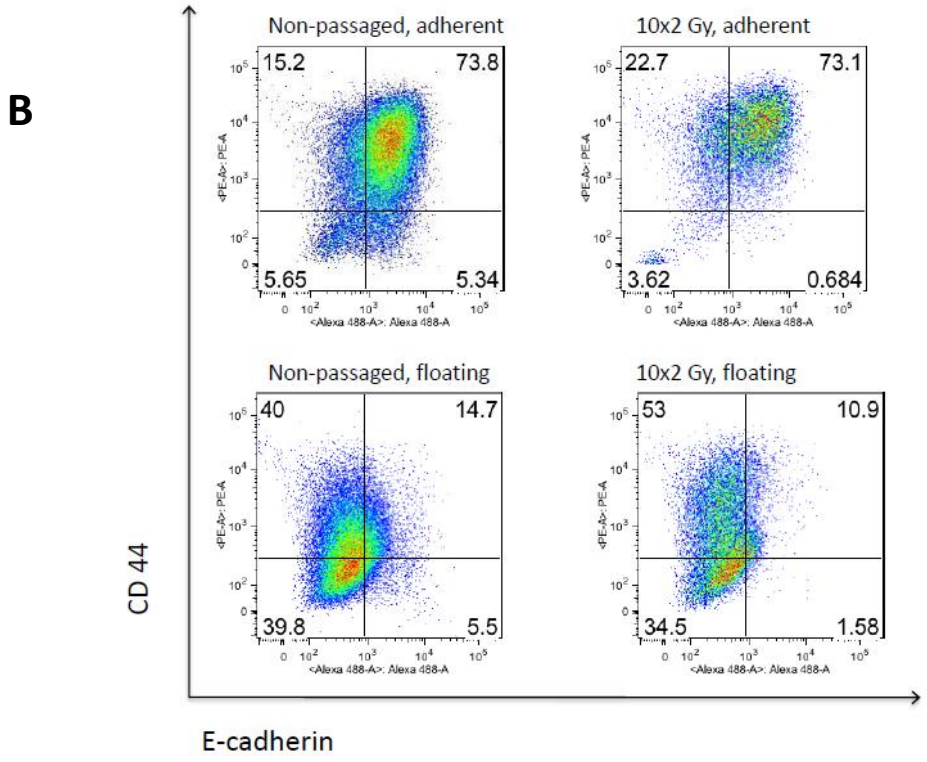

Figure 7: Expression of E-cadherin and CD44 in DU145 prostate cancer cell line, estimated by flow cytometry. Four examined fractions were: 1. control, non-irradiated and non-passaged adherent cells (up left); 2. five or ten times irradiated adherent cells (up right); 3. control, non-irradiated and non-passaged floating cells (down left); 4. five or ten times irradiated floating cells (down right). **A)** Five times irradiated cells; **B)** ten times irradiated cells.

After five days of irradiation, there was also a slight difference between control and irradiated samples, as both 5 times irradiated adherent cells and 5 times irradiated floating cells were more E-cadherin positive than control adherent cells and control floating cells, respectively. However, this difference was not observed 10 days after irradiation (Fig. 7, 8).

When comparing irradiated and control cells in respect of CD44 expression, we found that all irradiated cells had slightly higher levels of the CD44 antigen than control cells, in both adherent and floating fractions. Particularly, control floating fractions (after five and ten days) were CD44 negative, while their irradiated floating counterparts (five and ten times irradiated) were CD44 low. Interestingly, there was a huge difference between adherent and floating fractions, as all adherent fractions were highly CD44 positive, whereas all floating fractions were CD44 low or negative (Fig. 7).

To detect the stem cell subpopulation within each fraction, we used the CD49f antigen. However, there was always only one population of cells, ranging from CD49f high to CD49f low, so we could not use this marker for stem cell identification. Nevertheless, we noticed a substantial loss of CD49f in floating fractions in a comparison with respective adherent fractions. Furthermore, there was a slight difference between five times irradiated and relevant control cells, with the 5dIR adherent and 5dIR floating cells expressing more of the antigen than 5dCTRL adherent and 5dCTRL floating cells, respectively (Fig. 8).

The last marker, CD133, also turned out not to be useful for further analysis, because there was only one population of cells expressing this marker (data not shown).

To sum up, floating cells in both irradiated and control DU145 populations seem to downregulate expression and/or maintenance of E-cadherin, CD44 and CD49f antigens on the cell surface. Nevertheless, the expression of CD44 in floating cells seems to be maintained if not even induced after radiation treatment. This is in contrast to untreated floating cells, where the presence of CD44 declines over a time course of 10 days (Fig. 9). The expression of the other two antigens, E-cadherin and CD49f, in floating cells seems to be maintained/induced only after five days of radiation treatment.

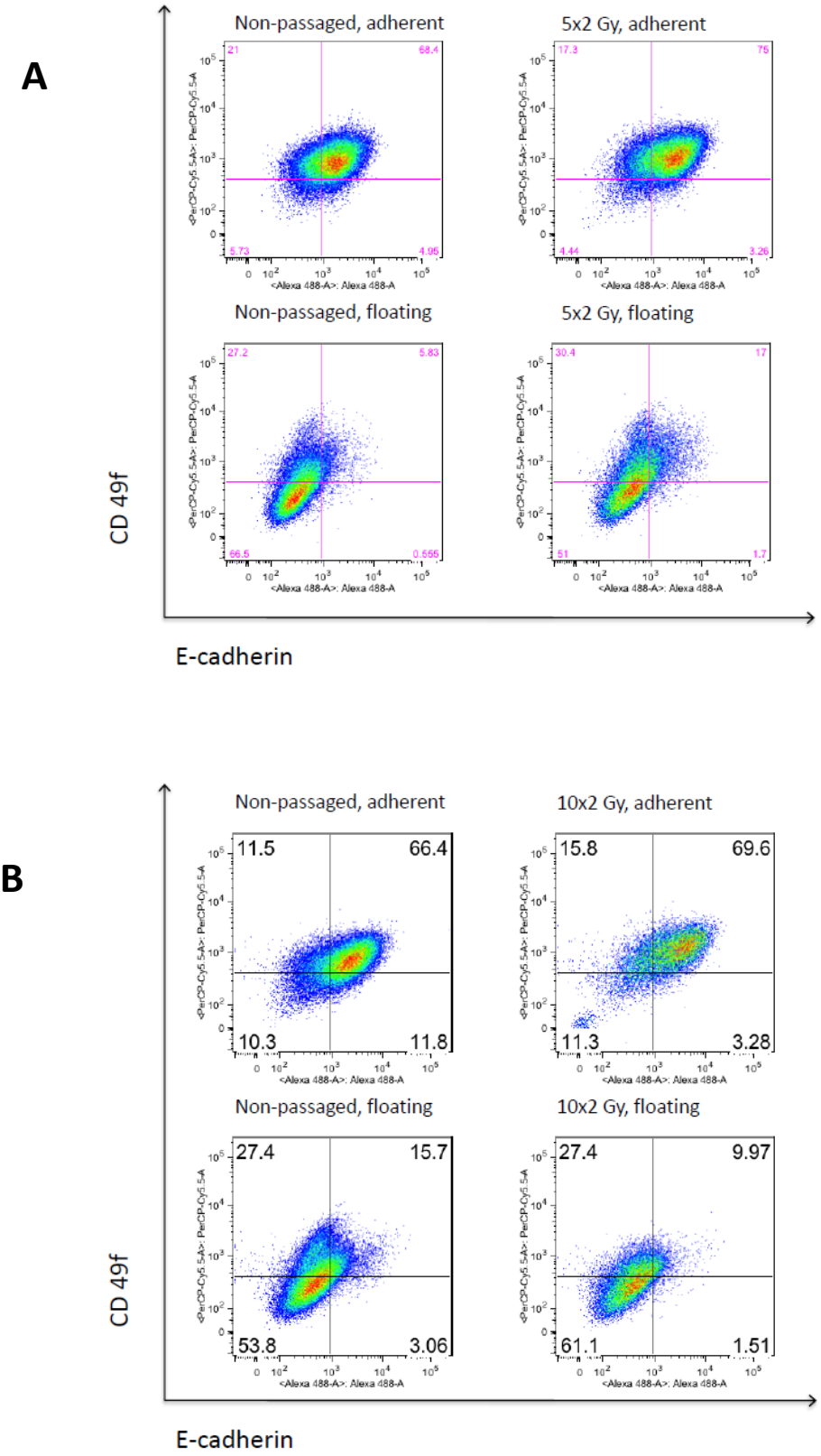

Figure 8: Expression of E-cadherin and CD49f in DU145 prostate cancer cell line, estimated by flow cytometry. Four examined fractions were: 1. control, non-irradiated and non-passaged adherent cells (up left); 2. five or ten times irradiated adherent cells (up right); 3. control, non-irradiated and non-passaged floating cells (down left); 4. five or ten times irradiated floating cells (down right). **A)** Five times irradiated cells; **B)** ten times irradiated cells.

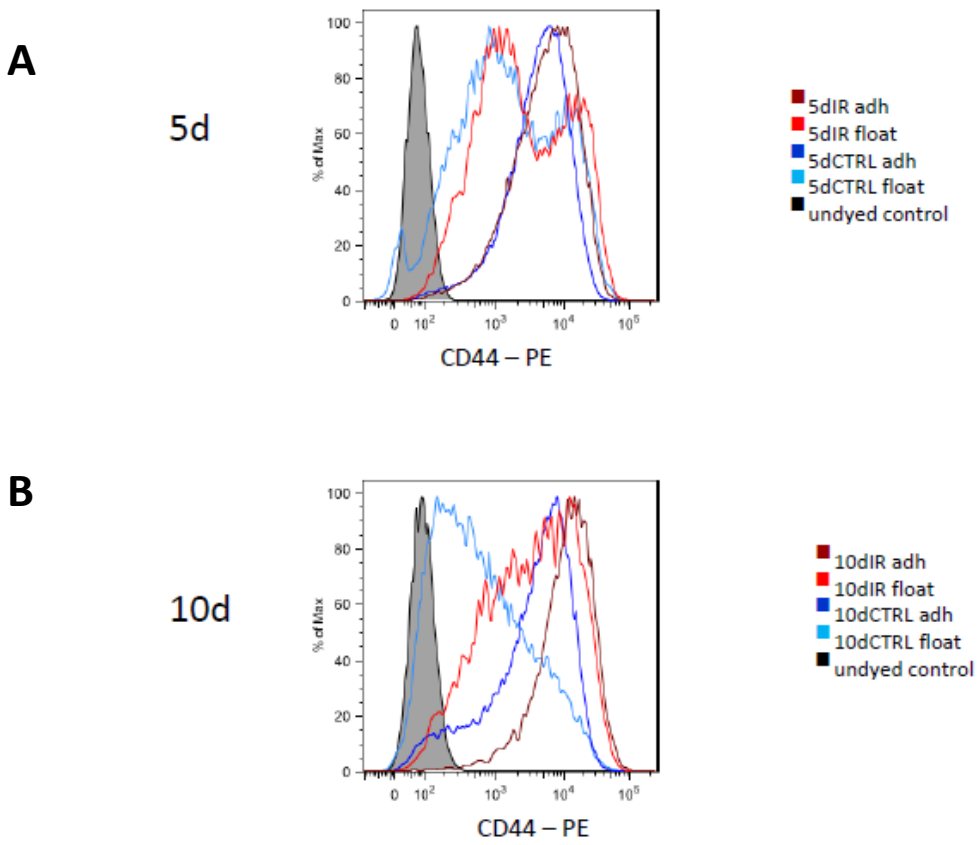

Figure 9: Fluorescence intensity histograms for CD44 antigen. Fluorescence intensity of CD44 antibody (PE channel) in IR adh, IR float, CTRL adh and CTRL float fractions of DU145 cells after **A)** 5 doses **B)** 10 doses of 2 Gy ionizing radiation.

3.5. Radiation causes cell cycle arrest

To follow cell proliferation, we used a dye eFluor 670 that unspecifically binds membrane proteins. Fluorescence intensity per cell should be maximal immediately after dyeing, and it should decrease approximately by 50% after each cell division, as the dyed membrane proteins dilute by newly synthesized, undyed ones.

To monitor cell proliferation during irradiation, we dyed normally cultured DU145 cells with cell proliferation dye and irradiated them with five or ten doses of 2 Gy ionizing radiation. Then we harvested floating and adherent cells separately and measured fluorescence intensity of proliferation dye in these fractions.

After five days of irradiation, there was almost no difference between the fractions. When comparing irradiated floating fraction and control floating fraction, the fluorescence intensity was almost the same (Fig. 10A) and similarly, when comparing irradiated adherent fraction to control

adherent fraction, we detected only slightly higher proliferation rate in control cells (Fig. 10B). However, in both irradiated and control populations, the adherent fractions proliferated faster than the floating fractions (Fig. 10C, D). Interestingly, after ten days of irradiation the results were different and we observed a clear difference between irradiated and control samples, as control cells proliferated more efficiently than irradiated ones (Fig. 11A, B).

Focusing on the two fractions within each population, we noticed, that in control cells there almost disappeared the difference in fluorescence intensity between adherent and floating fraction, which was so evident after five days (Fig. 11D). In irradiated cells the difference remained, however only in the right part of the histogram (Fig. 11C). We give some explanations in a Discussion.

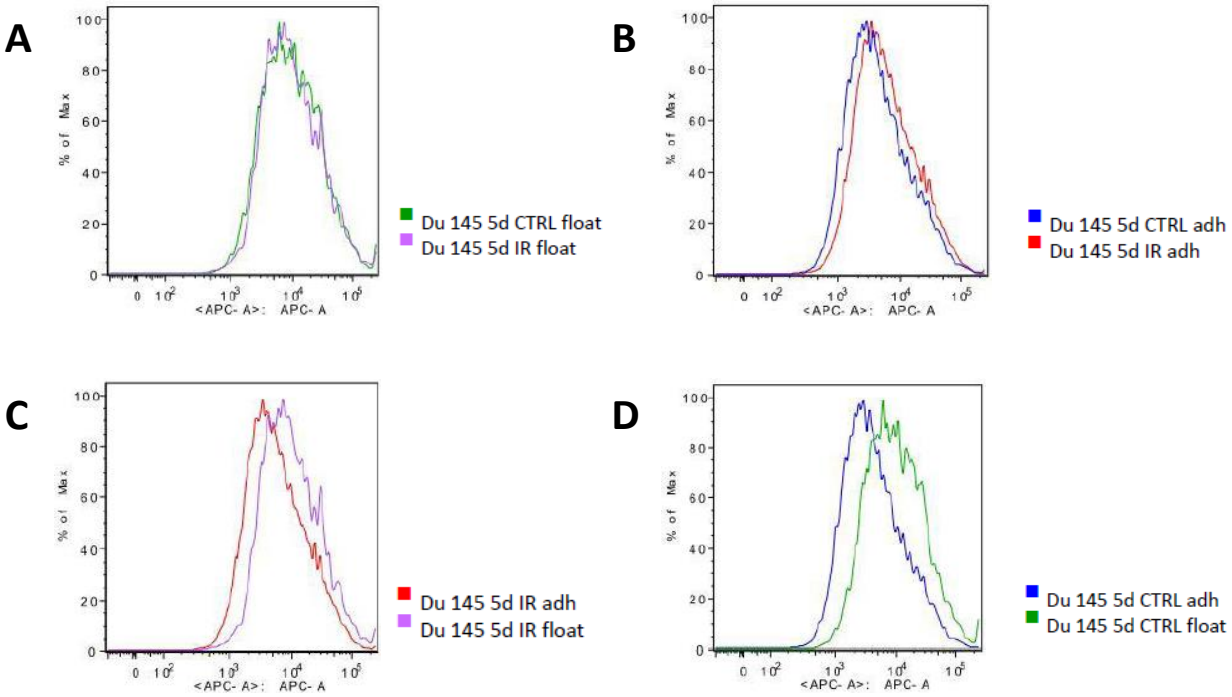

Figure 10: Estimation of cell proliferation in 5 times irradiated cells. Fluorescence intensity histograms for Cell proliferation dye eFluor 670 (APC channel). Comparison of **A)** control floating fraction and irradiated floating fraction; **B)** control adherent fraction and irradiated adherent fraction; **C)** irradiated adherent fraction and irradiated floating fraction; **D)** control adherent fraction and control floating fraction.

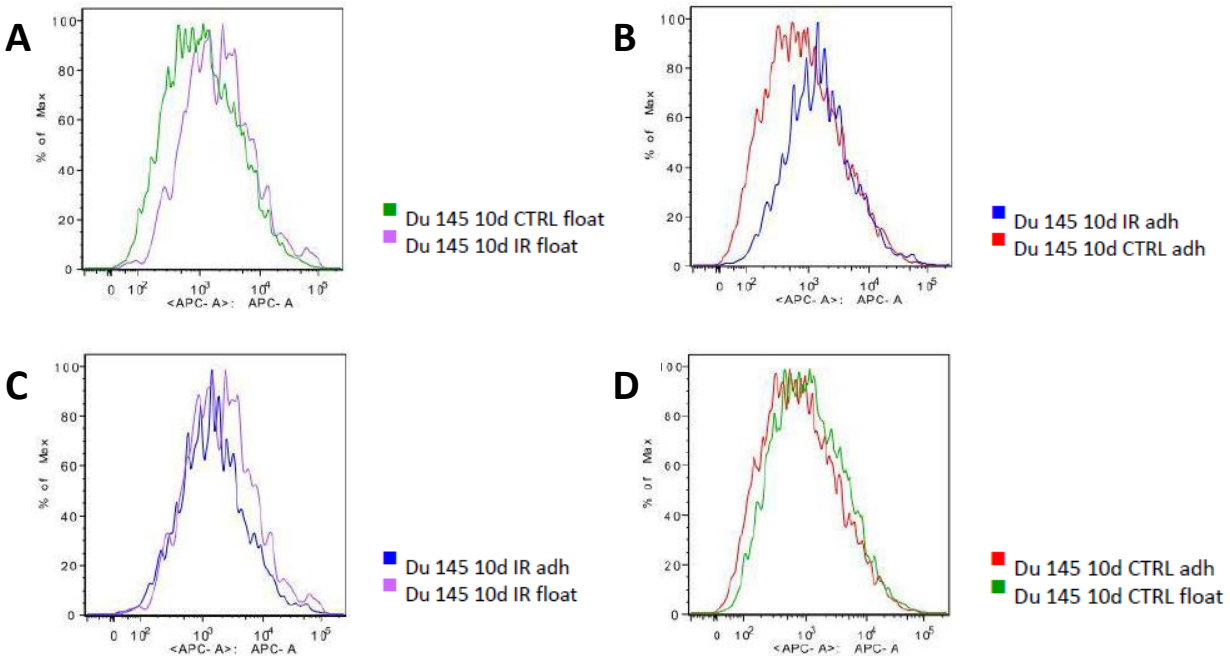

Figure 11: Estimation of cell proliferation in 10 times irradiated cells. Fluorescence intensity histograms for Cell proliferation dye eFluor 670 (APC channel). Comparison of **A)** control floating fraction and irradiated floating fraction; **B)** control adherent fraction and irradiated adherent fraction; **C)** irradiated adherent fraction and irradiated floating fraction; **D)** control adherent fraction and control floating fraction.

3.6. Cell cycle profile of irradiated cells

When examining cell proliferation, we found that radiation causes proliferation slowdown or even arrest. To determine in which phase of their cycle are the cells arrested, we dyed the cell DNA with propidium iodide, measured its content in individual cells and generated cell cycle profile by flow cytometry.

First we focused on adherent cells and we ascertained, that five and ten times irradiated cells are enriched in G2/M phase, while the G2/M peak of ten times irradiated cells was approximately twice as high as that of five times irradiated cells (Fig. 12B).

Then we looked on floating cells and the first thing we noticed was significant enrichment in S phase and G2/M phase in all four floating fractions (five and ten times irradiated and respective control floating fractions). The S plateau and G2/M peak were not so marked in control floating cells after ten days, which means that the cell cycle profile of this fraction was closest to the profile of adherent cells (Fig. 12B). We suggest some explanations of this phenomenon in Discussion. Furthermore, we observed that the G2/M peak was again much higher in irradiated cells than in controls, analogously to the situation among adherent fractions (Fig. 12A, B).

To conclude, all irradiated cells are arrested in G2/M phase of their cell cycle. The percentage of arrested cells is much higher in floating cells, which are furthermore enriched in S phase.

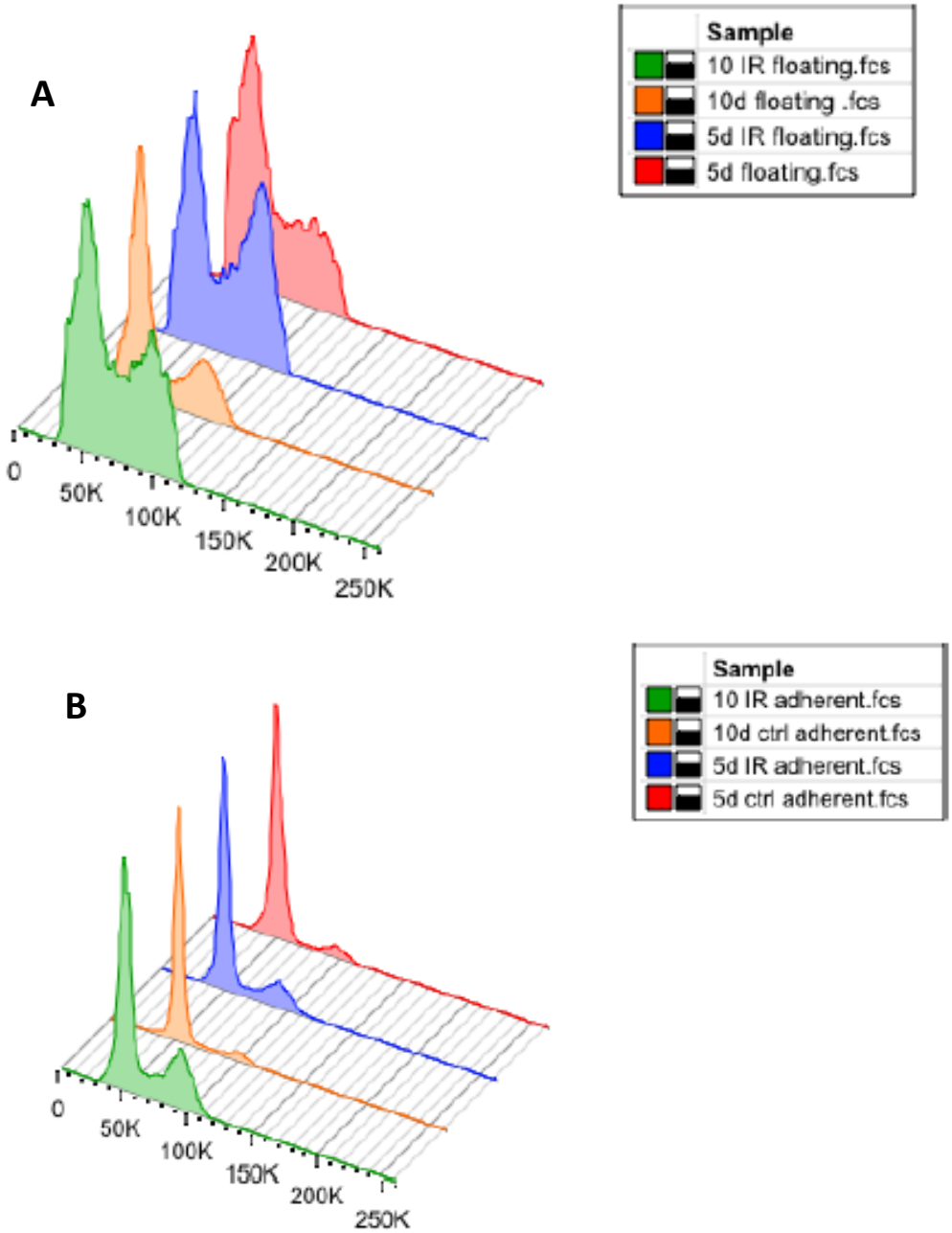

Figure 12: Cell cycle profile analysis by flow cytometry. A) Floating cells – 5 times irradiated and respective controls, 10 times irradiated and respective controls. **B)** Adherent cells – 5 times irradiated and respective controls, 10 times irradiated and respective controls.

3.7. Irradiated floating cells need to readhere to restart proliferation

To follow cell proliferation in floating and readherent cells for certain period after the end of irradiation, we again used the cell proliferation dye eFluor 670. We dyed the floating fractions of both irradiated and control cells on the same day when they received their last, tenth dose of 2 Gy. The fluorescence intensity was measured immediately after dyeing and later on at four selected time points (6 days, 12 days, 20 days and 28 days after dyeing). When we focused only on the cells that still floated in medium throughout all the timepoints, we observed a clear difference: in the control floating fraction the fluorescence intensity decreased with time indicating cell proliferation (Fig. 13A); in the irradiated floating cell fraction, on the other hand, the fluorescent intensity remained almost the same which indicated cell cycle arrest (Fig. 13B).

However, approximately 20 days after dyeing, part of the irradiated floating cells reattached. When analyzed, some of the readherent cells turned out to proliferate normally, as there were several peaks for various fluorescence intensities on the graph, ranging from more than 10^4 to 0 (Fig. 14A).

28 days after dyeing, the proliferation dye on irradiated readherent cells was completely diluted out, showing efficient proliferation, whereas fluorescent intensity for irraddiated floating cells at the same time point was still more than 10^4 (Fig. 14B).

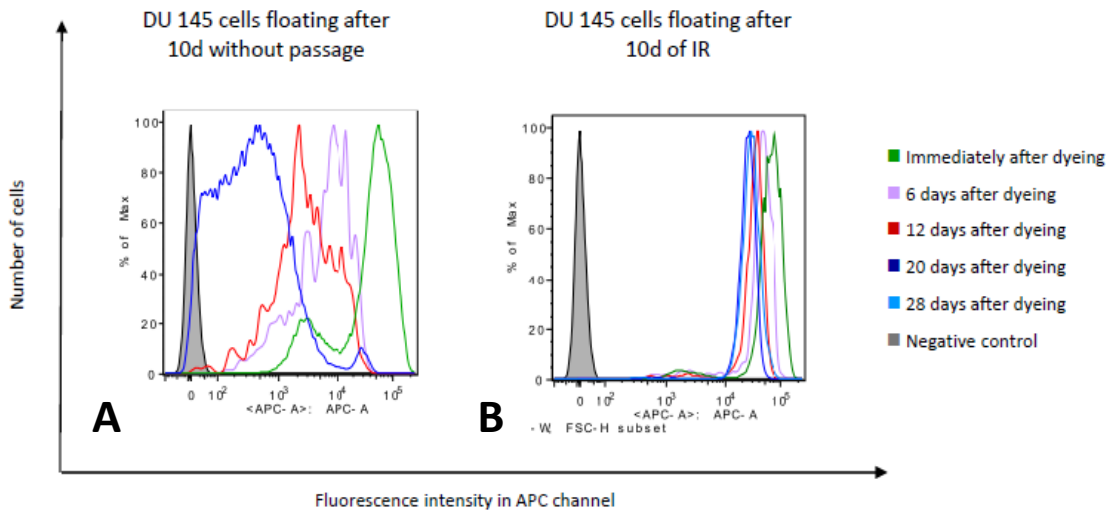

Figure 13: Estimation of cell proliferation after irradiation. Fluorescence intensity histograms for Cell proliferation dye eFluor 670 (APC channel) – floating cells. Cells that started floating after 10 days without/with radiation were dyed by Cell proliferation dye eFluor 670 and fluorescence intensity was measured at selected time points. **A) c**ells floating without radiation; **B)** cells floating after receiving 10 doses of 2Gy ionizing radiation.

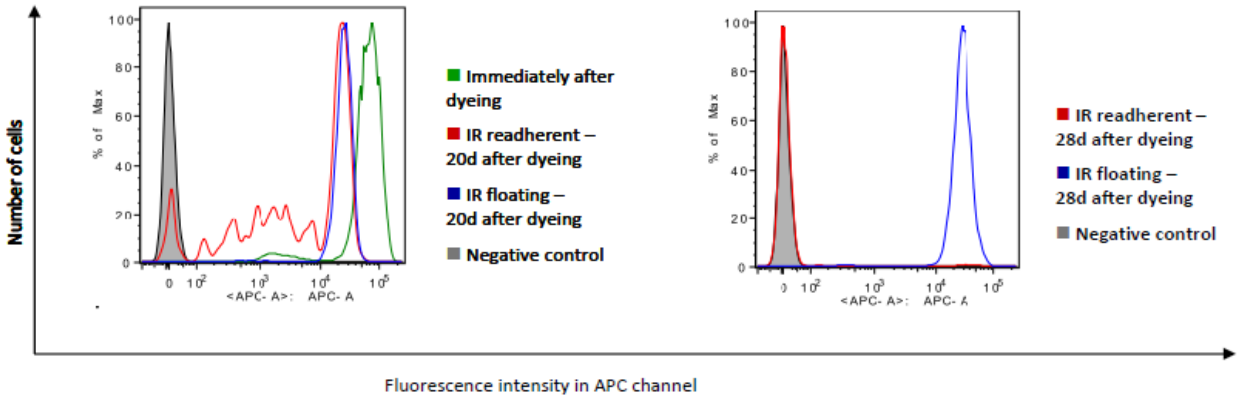

Figure 14: Comparison of cell proliferation after irradiation. Fluorescence intensity histograms for Cell proliferation dye eFluor 670 (APC channel) – floating cells vs readherent cells. Cells that started floating after 10 days without/with radiation were dyed by Cell proliferation dye eFluor 670 and fluorescence intensity was measured at selected time points. From certain time points some cells adhered back to the dish surface. These cells were analyzed separately from the floating fraction as so called readherent fraction. This figure shows fluorescence intensity of proliferation dye in floating vs readherent cells **A)** 20 days after dyeing; **B)** 28 days after dyeing.

To conclude, non-irradiated cells proliferated normally, no matter whether they are floating or adherent (Fig. 13A, 15A). On the contrary, irradiated cells do not proliferate while floating and they have to readhere to restart proliferation (Fig. 13B, 15B).

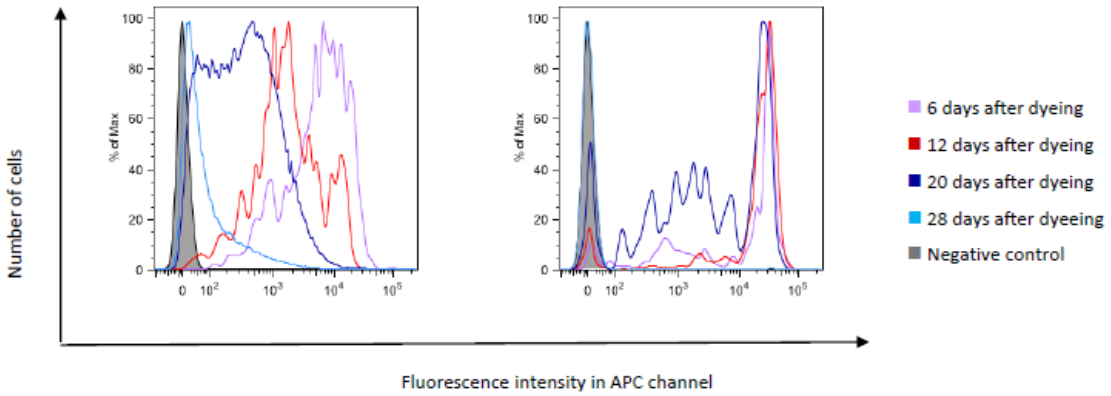

Figure 15: Comparison of cell proliferation in readherent cells. Fluorescence intensity histograms for Cell proliferation dye eFluor 670 (APC channel) – readherent cells – control vs irradiated. Cells that started floating after 10 days without/with radiation were dyed by Cell proliferation dye eFluor 670 and fluorescence intensity was measured at selected time points. From certain time points some cells adhered back to the dish surface. These cells were analyzed separately from the floating fraction as so called readherent fraction. This figure shows fluorescence intensity of proliferation dye in readherent cells, that originated from **A)** control, non-irradiated cells; **B)** ten times irradiated cells.

3.8. Vimentin and E-cadherin expression in readherent cells

We wanted to see what happens with DU145 cells that started floating after irradiation, when they readhere back to the surface. For this purpose we let the cells readhere for several days, then we treated them with Versene and seeded onto eight-chamber culture slides (see Materials and Methods). After two days we stained them for immunofluorescence. As non-irradiated control we took normally cultured DU145 cells, which were passaged regularly.

By immunofluorescence we could observe an increase in vimentin expression in readherent cells (Fig. 16A). Furthermore we detected marked change in E-cadherin localization, as control cells had most of their E-cadherin on a membrane, whereas E-cadherin in readherent cells was localized primarily into nucleus (Fig. 16B). We give some possible explanations of these results in a Discussion.

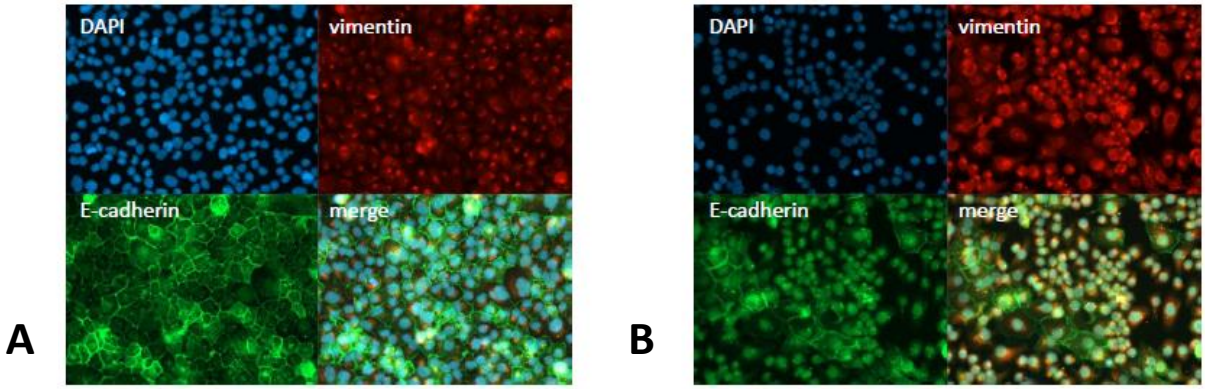

Figure 16: Vimentin and E-cadherin expression estimated by immunofluorescence. A) Control cells; **B)** readherent cells.

3.9. E-cadherin, CD44 and CD49f expression in readherent cells estimated by flow cytometry

As a next step we wanted to describe changes in E-cadherin, CD44 and CD49f expression in DU145 readherent cells compared to adherent and floating control populations by flow cytometry.

Focusing first on E-cadherin, we revealed, that the protein levels are much lower in readherent cells than in control adherent population (Fig. 17B, C, H, I); in fact, they are more related to those of floating cells (Fig. 17E, F). Based on flow cytometry results, it might therefore seem that overall E-cadherin expression is decreased in readherent cells. However, flow cytometry (at least as it was performed in our study) can only measure membrane-localized fraction

of the protein and thus it is very useful to analyze the FACS data together with the results, that we got using immunofluorescence staining. In the immunofluorescence pictures we can see, that E-cadherin expression is not significantly changed (Fig. 16 A, B). What is changed, is the localization of this protein, as it is translocated from membrane into nucleus.

In case of CD44 antigen, the situation was analogical; the expression pattern of DU145 readherent cells much more resmbled that one of floating cells than that one of adherent control cells. Whereas in adherent control sample almost all cells were CD44 positive, in readherent sample, as well as in floating sample, approximately half of the cells was CD44 positive and the other half CD44 negative (Fig. 17B, E, H).

Interestingly, the results were opposite, while looking at CD49f expression. Here most of the adherent control population was CD49f positive, just as the readherent cells, whereas most of the floating controls were CD49f negative (Fig. 17C, F, I). We try to interpret these results in a Discussion as well.

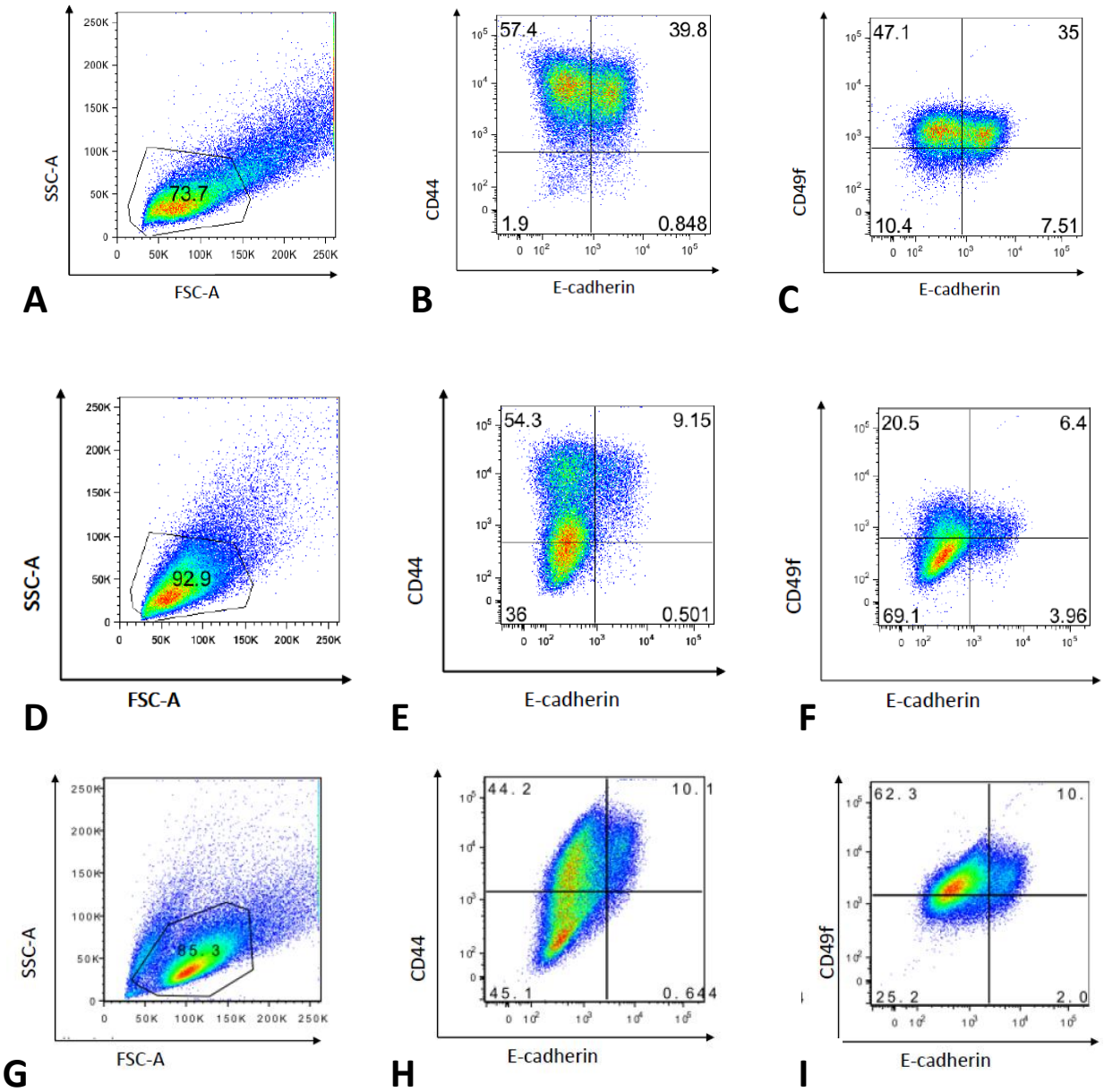

Figure 17: Expression of E-cadherin, CD44 and CD49f in DU145 cells estimated by flow cytometry. A) Population of DU145 adherent control cells; **B)** expression of E-cadherin and CD44 in DU145 adherent control cells; **C)** expression of E-cadherin and CD49f in DU145 adherent control cells; **D)** population of DU145 floating control cells; **E)** expression of E-cadherin and CD44 in DU145 floating control cells; **F)** expression of E-cadherin and CD49f in DU145 floating control cells; **G)** population of DU145 readherent cells; **H)** expression of E-cadherin and CD44 in DU145 readherent cells and **I)** expression of E-cadherin and CD49f in DU145 readherent cells.

4. Discussion

The goal of this project was to characterize the prostate tumor cells after radiation treatment which closely resembles patients treatment during radiotherapy. We suggested a hypothesis that γ-radiation causes changes in cell phenotype, mainly in the area of epithelial-to-mesenchymal transition and cell dedifferentiation, i.e. stem-like state. Therefore, we examined the expression of selected mesenchymal and stem cell markers in adherent cell fraction following irradiation. Furthermore, we focused on the cells that started floating after irradiation but did not succumb to anoikis; especially we were interested whether these cells are proliferating and what does their cell cycle profile and look like.

We showed that there are no significant changes in epithelial/mesenchymal character of the cells after radiation treatment. However, the cells in irradiated floating fractions are, at least to certain extent, able to maintain expression of CD44 and CD49f, contrary to control floating cells, where the expression of these markers rapidly decreases after the cells detach from surface. When examining the phenotype of readherent cells, we found out that it is somewhere between the phenotype of parental adherent and floating cells. In the second part of this project we described, that in contrast to non-irradiated floating cells the irradiated floating cells do not proliferate and they are only able to restart proliferation when they reattach. Moreover, in contrast to non-irradiated floating cells, the irradiated floating cells do not proliferate but they are able to restart proliferation after they reattach. Finally we described occurence of G2/M cell cycle arrest in irradiated cells.

4.1. Expression of selected epithelial, mesenchymal and stem cell markers in control cells

When examining the expression of selected mesenchymal and stem cell markers in PC-3 and DU145 cell lines by immunofluorescence and flow cytometry, we revealed, that PC-3 cell line demonstrates more mesenchymal phenotype than DU145 cell line. This is in concert with previous reports, when expression of mesenchymal proteins N-cadherin and cadherin-11 was detected in PC-3 cells but not in DU145 cells (Murali et al. 2012), suggesting that PC-3 cells are overall more mesenchymal. We further noticed that there were two different populations of PC-3 cells regarding E-cadherin and β-catenin expression. DU145 cell line was more uniform, nevertheless, even here we detected two populations of cells: one being E-cadherin/β-catenin negative or low, the other being E-cadherin/β-catenin high. Such a heterogeneity is not unusual in malignant epithelial cell lines and has been attributed either to genetic instability and clonal evolution (Weiss 2000), or to the

hierarchical patterns of normal epithelium, which seem to be maintained in epithelial malignancies, as well as in carcinoma-generated cell lines (Locke et al. 2005, van Bokhoven et al. 2003).

Concerning DU145 cancer cell line, it is known, when plated at clonal densities, it forms three typical clonal morphologies represented by holoclones (compact round colonies), meroclones (intermediate features), and paraclones (loose irregular colonies; Webber et al. 1997, Locke et al. 2005). Importantly, whereas cells in holoclones are small and senescence-associated β-galactosidase (SA-beta-gal) negative, most cells in paraclones are flat, large and SA-βgal positive, suggesting that the latter cells are mostly senescent and nonproliferative (Li et al. 2008). Besides, it has been shown for DU145 holoclones, that they have higher clonogenicity than the other two clones, and in contrast to paraclones or meroclones, their constituent cells can give rise to all three types of clones. Together it indicates that the cells in holoclones are less differentiated and more stem-like than the cells in the other two clone types (Locke et al. 2005). In addition, expression profile of the three clone types differs, of particular interest being higher expression of β1 integrin, β-catenin or E-cadherin by the cells of holoclones (Locke et al. 2005). Thus, it is possible, that higher E-cadherin expression in cells of holoclones predisposes these cells to stay attached to the surface, in contrast to E-cadherin low cells of paraclones or meroclones.

As for PC-3 cells, the occurrence of the same three types of clones has been noted, with the same morphological patterns (compact colonies, smaller cells and SA-βgal negative staining in holoclones). As well as in DU145 cells, the cells in holoclones seem to be more stem-like, with higher tumorigenicity and serial tumor transplantation sustainability. Furthermore, holoclones express high levels of stem and progenitor cell markers CD44, α2β1 integrin, and β-catenin (Li et al. 2008).

Hence, our observation of differential E-cadherin and β-catenin expression can be attributed to this population heterogeneity within both cell lines.

Other explanation of differential E-cadherin expression lies in a common slight difference in proliferation rate between individual cells in culture. The more proliferative areas have higher cell density, the cells in these areas are smaller and overall E-cadherin expression related to certain area arises. Nevertheless, it is still possible that higher proliferation rate is inherent property of certain subpopulation of cells (e.g. cells forming holoclones at clonal density). What is interesting, the cells that were cultured for 5 or 10 days without passaging (both control and irradiated) showed almost homogenous E-cadherin expression. Possible explanation could be, that the cells which divided faster at the beginning of cultivation, are partly contact-inhibited after a few days without passage, and so the cells with slower proliferation rate can grow into equal density in the meantime. Equal density then means equal E-cadherin levels related to certain area.

4.2. Expression of selected mesenchymal and stem cell markers decreases in floating cell fraction, but ionizing radiation seems to counteract this process

When we measured the post-irradiation levels of E-cadherin, CD44 and CD49f by flow cytometry, we found out that in all examined fractions there were no more two populations of cells regarding E-cadherin expression but only one. This correlates with the immunofluorescence findings, where we could observe more homogenous E-cadherin distribution after 5 and 10 days of culturing. It seems again that confluent cells somehow lose E-cadherin heterogeneity, possibly due to equalization of their density. Surprisingly, we did not spot any decrease in E-cadherin levels in irradiated cells, although such a decrease has been described for other cells previously (Park et al. 2003, De Carvalho et al. 2006).

By FACS analysis we further described that floating cells seem to downregulate expression and/or maintenance of E-cadherin, CD44 and CD49f surface antigens. There might be multiple reasons for that observation. First of all, it is important to note that all the three molecules, including CD44 (Goodison et al. 1999), are originally cell surface adhesion molecules involved in cell-cell and cell-matrix interactions; thus it is not surprising that floating cells have lower levels of these antigens than adherent cells. What remains elusive is whether the cells have had lower E-cadherin, CD44 and CD49f levels from the beginning, thus forming weaker cell-cell and cell-surface interactions and starting to float as first among others, or whether there are some other factors causing cell detachment, and the decrease of adhesion molecules is merely secondary reaction. Whatever the answer is, radiation seems to counteract this process. The effect is most marked on CD44 expression after 5 doses of radiation, when control floating cells possess low CD44 expression upon floating, whereas irradiated floating cells are, at least to certain extent, able to maintain it. It might well be that without exposition to radiation only CD44-negative/low cells detach, whereas after irradiation also the CD44-medium/high cells are forced to detach by some other, radiation-induced mechanisms. However, recent article by Xiao et al. (Xiao et al. 2012) makes these results more interesting, while it describes association between CD44 expression and radioresistance in three prostate cancer cell lines (PC-3, PC-3M-luc and LNCaP). It is tempting to interpret higher CD44 expression in irradiated floating cells as a marker of higher radioresistance. With this presumption most of the floating cells would be killed by irradiation, they woul only be able to survive if their CD44 expression was somehow maintained. This would also explain the rapid disappearance of CD44 negative cells in adherent fractions after 5 and 10 doses of radiation. The only discrepancy is that after ten doses of radiation, CD44 level in irradiated floating cells decreases. According our

hypothesis it should be even higher than after five doses, as only the cells with the highest CD44 expression should now survive. Possible explanation is that after ten doses of radiation most of the floating cells are in advanced state of senescence and thus they lose all the surface molecules.

The results are very similar, though not so marked, for E-cadherin expression. Also for E-cadherin expression we observed a huge decrease in floating cells and – just as for CD44 expression – there are two explanations for that. Either the cells already have lower E-cadherin expression when they are adherent, and so they start floating earlier than E-cadherin-medium/high cells, or there are other stimuli causing general cell detachment and all the detached cells equally lower E-cadherin expression in response to that. Furthermore, analogically to CD44, E-cadherin expression in five times irradiated floating cells is higher than in control floating cells; however, after ten doses of radiation it is the opposite. The concept used in the case of CD44 (that floating cells are able to survive because of high CD44 expression) would therefore perfectly fit for E-cadherin, too, except of the fact that there are emerging data on correlation between low E-cadherin expression and radioresistance (Theys et al. 2011).

4.3. Radiation causes cell cycle arrest in G2/M phase

In the experiment with cell proliferation dye we showed, that irradiated cells proliferate slower than control cells and floating cells of each fraction slower than corresponding adherent cells. After five days the effect of radiation was relatively small – both adherent and control cells proliferated with similar rate – and it was overridden by the effect of floating, when irradiated and control floating cells proliferated slower than irradiated and control adherent cells, respectively. However, after ten days of irradiation it reversed: there was only a slight difference between adherent and floating cells, whereas there arose much bigger difference between irradiated cells and controls, while irradiated cells clearly proliferated less efficiently. This is in agreement with previous reports documenting delayed cell growth and division after radiation treatment (Vucić et al. 2006, Skvortsova et al. 2008). There is just one more detail which needs to be commented: why is there a difference in the right part of the histogram between irradiated adherent and floating fractions after ten doses of irradiation (Fig. 11 C), when such a difference is not detectable in control cells (Fig. 11 D)? If we accept that irradiated cells do not proliferate when they start floating but control cells do, the explanation is easy. The left part of the histogram is identical for both fractions, because some of the floating cells started to float very recently and for most of their time they have been dividing just as adherent cells. But the right part of the histogram shows that whereas all

adherent cells proliferate constantly, those floating cells which started to float earlier also stopped dividing earlier and “stood behind”.

Next, we focused only on the floating fraction that we obtained after ten days with or without irradiation. We replated these cells onto a new dish, dyed them with cell proliferation dye and followed their proliferation. The first thing we noted was that the control floating cells created readherent fraction within a few days, whereas irradiated cells needed almost one month to readhere. We further observed, that the floating fraction of irradiated cells did not proliferate at all during the duration of the experiment; the slight decrease in fluorescence intensity (Fig. 13 B) was most likely due to the detaching and washing steps foregoing every FACS analysis. On the contrary, non-irradiated floating cells proliferated normally; even though we have to admit that it is difficult to distinguish, whether the cells divide while floating or whether they need to attach to the surface to divide and after some time they start floating again. As a next step we examined the readherent fraction that originated from the floating cells and we found out that both control and irradiated cells do proliferate when they readhere. Thus we can speculate that either the control cells are able to divide while floating whereas the irradiated cells need to readhere to accomplish cell division; or that both control and irradiated cells have to be attached to proliferate, but control cells are able to do it, whereas irradiated cells – for some reason – are not. One of the reasons might be that irradiated cells are busy repairing their DNA, which was damaged by radiation. Further experiments are needed to fully elucidate this phenomenon.

In order to pin down the problem, we began with cell cycle profile analysis of all the fractions gained during irradiation. We ascertained that all irradiated cells are arrested in G2/M phase and the fraction of arrested cells is much higher in floating cells than in adherent ones. There was no peak in G1 phase of the cell cycle, since DU145 cells have mutated p53 protein and are therefore not able to arrest in G1, which was already described by Böhnke et al. (Böhnke et al. 2004). So far it supports our hypothesis that the DNA of irradiated floating cells is damaged seriously and the cells are not able to readhere and restart proliferation unless they repair it. Yet we would like to discuss why the cell cycle profile of control floating cells after ten days closely resembles that one of adherent cells. We think, that after ten days the culture is already over confluent and the cells released to medium are more or less the same as the cells which stay attached, there is just not enough space for them to stay attached. It is in consensus with the results that we got from cell survival experiments (Fig. 3B).

4.4. Expression of selected epithelial, mesenchymal and stem cell markers in readherent cells

To better characterize the post-irradiated readherent cells, we performed immunofluorescence staining and FACS analysis for selected epithelial, mesenchymal and stem cell markers.

By immunofluorescence we could observe an increase in vimentin expression in readherent cells, which might suggest that vimentin levels increase not only in irradiated adherent cells, but also in irradiated floating cells, from which the readherent cells originate. E-cadherin in readherent cells was localized mostly into nucleus, whereas in control cells it appeared primarily on the membrane. There are several ways how to explain this. Firstly, we have showed here, that cells upon floating underwent kind of epithelial to mesenchymal transition, losing most of their membrane E-cadherin (Fig. 7, 8). Nevertheless it has not been clear, whether the protein was degraded entirely or whether it was merely internalized. In the immunofluorescence image we can see that E-cadherin levels in irradiated readherent cells are not substantially decreased compared to controls, but the protein has been translocated from membrane to the nucleus. Therefore, we can speculate that during loss of adhesion E-cadherin is cleaved and transported to the nucleus and when the cells readhered, it may take them longer to restore adherens junctions between each other, including transport of E-cadherin to membrane. The second possible explanation for the change in E-cadherin localization may be the detaching step foregoing immunofluorescence analysis. For sure there must be something special about the irradiated floating cells, since it takes them almost one month to create readherent culture, whereas control floating cells readhere and efficiently proliferate already after a few days. On the other hand, once the irradiated floating cells readhere, it is very difficult to detach them from the surface. We treated the cells on dishes with versene to be able to seed them onto culture slides for immunofluorescence. And whereas it took 45 minutes to normally cultured cells to detach, we had to wait almost two hours until the irradiated readherent cells detached. During this prolonged detaching, cells might have lost most of their membrane E-cadherin, even though they might have had it present when growing on the dish.

By flow cytometry we showed that the phenotype of readherent cells is somewhere between adherent and floating cells. The expression pattern of E-cadherin and CD44 more resembled that of floating cells, but in both cases there was a small subpopulation leaning to the adherent-like pattern. In the case of CD49f, its expression was somewhere in the middle – neither positive as

in adherent fraction, nor negative as in floating cells. We already tried to explain this “intermediate phenotype” for E-cadherin above, and similar reasoning can be used for the other two antigens.

5. Conclusion

In this thesis we have pinned down some changes in cell phenotype, occurring after fractionated radiation treatment. We have also described cell cycle arrest in the floating fraction of irradiated cells and showed that the arrest is not permanent, while the cells are able to reenter cell cycle when they readhere. In other experiments performed in our laboratory we showed elevated expression of the key mesenchymal inducer Snail1 in irradiated floating cells.

Based on these data we suggest a possible mechanism by which the CaP cells survive radiation and either restore original tumor or metastasize to distant locations. We propose that radiation induces at least partial EMT transition in the irradiated cells, enabling some cells to detach from the tumor tissue without anoikis. These detached cells remain arrested in G2/M phase unless they find a suitable niche for readhesion and proliferation restart.

To confirm this hypothesis more data are needed to prove EMT in irradiated floating cells.

Follow-up objective is to reveal signaling events underlying EMT process and cell cycle arrest. Knowing the key signal components of radiation-induced pathways which allow the tumor cells to survive the radiation treatment, we could be able to develop inhibitors targeting them specifically, thus lowering post-radiation survival and subsequent progression to advanced disease.

6. Resources

Books

Greger R, Windhorst U. Comprehensive human physiology: from cellular mechanisms to intagration. Springer-Verlag Berlin Heidelberg 1996. ISBN 3-540-58109-X.

Vander AJ, Sherman JH, Luciano DS. Human Physiology, The Mechanisms of Body Function. McGraw-Hill 1990. ISBN 0-07-066969-4.

Russell PJ, Jackson P, Kingsley EA. Prostate Cancer Methods and Protocols (Methods in Molecular Medicine). Humana Press 2003. ISBN-10: 0896039781.

Journals

Abell AN, Jordan NV, Huang W, Prat A, Midland AA, Johnson NL, Granger DA, Mieczkowski PA, Perou CM, Gomez SM, Li L, Johnson GL. MAP3K4/CBP-regulated H2B acetylation controls epithelial-mesenchymal transition in trophoblast stem cells. Cell Stem Cell 2011; 8(5): 525-37.

Abdulghani J, Gu L, Dagvadorj A, Lutz J, Leiby B, Bonuccelli G, Lisanti MP, Zellweger T, Alanen K, Mirtti T, Visakorpi T, Bubendorf L, Nevalainen MT. Stat3 promotes metastatic progression of prostate cancer. Am J Pathol 2008 Jun; 172(6): 1717-28.

Agarwal N, Sonpavde G, Sternberg CN. Novel molecular targets for the therapy of castration-resistant prostate cancer. Eur Urol 2012; 61(5): 950-60.

Aigner K, Dampier B, Descovich L, Mikula M, Sultan A, Schreiber M, Mikulits W, Brabletz T, Strand D, Obrist P, Sommergruber W, Schweifer N, Wernitznig A, Beug H, Foisner R, Eger A. The transcription factor ZEB1 (deltaEF1) promotes tumor cell dedifferentiation by repressing master regulators of epithelial polarity. Oncogene 2007; 26(49): 6979-88.

Amaral TM, Macedo D, Fernandes I, Costa L. Castration-resistant prostate cancer: mechanisms, targets, and treatment. Prostate Cancer 2012; 2012: 327253.

Aneja S, Pratiwadi RR, Yu JB. Hypofractionated radiation therapy for prostate cancer: risks and potential benefits in a fiscally conservative health care system. Oncology 2012; 26(6): 512-8.

Armstrong AJ, Oltean S, Marengo M, Chen L, Kemeny G, Herold CI, Marcom PK, George DJ, Garcia-Blanco M. Plasticity, stemness, and aggressive behavior in preclinical models and circulating prostate cancer cells: importance of the transitional phenotypic state to lethal cancer biology. Proceedings of the Genitourinary Cancers Symposium; 5–7 March 2010; San Francisco, CA, USA. ASCO: Alexandria, VA, USA, 2010, abstract 172.

Attard G, Sarker D, Reid A, Molife R, Parker C, de Bono JS. Improving the outcome of patients with castration-resistant prostate cancer through rational drug development. Br J Cancer 2006; 95(7): 767-74.

Bachelder RE, Yoon SO, Franci C, de Herreros AG, Mercurio AM. Glycogen synthase kinase-3 is an endogenous inhibitor of Snail transcription: implications for the epithelial–mesenchymal transition. J Cell Biol 2005; 168: 29-33.

Barreto-Andrade JC, Efimova EV, Mauceri HJ, Beckett MA, Sutton HG, Darga TE, Vokes EE, Posner MC, Kron SJ, Weichselbaum RR. Response of human prostate cancer cells and tumors to combining PARP inhibition with ionizing radiation. Mol Cancer Ther 2011; 10(7): 1185-93.

Batlle E, Sancho E, Francí C, Domínguez D, Monfar M, Baulida J, García De Herreros A. The transcription factor snail is a repressor of E-cadherin gene expression in epithelial tumor cells. Nat Cell Biol 2000; 2(2): 84-9.

Behnsawy HM, Miyake H, Harada K, Fujisawa M. Expression patterns of epithelial-mesenchymal transition markers in localized prostate cancer: significance in clinicopathological outcomes following radical prostatectomy. BJU Int 2013; 111(1): 30-7.

Berger MF, Lawrence MS, Demichelis F, Drier Y, Cibulskis K, Sivachenko AY, Sboner A, Esgueva R, Pflueger D, Sougnez C, Onofrio R, Carter SL, Park K, Habegger L, Ambrogio L, Fennell T, Parkin M, Saksena G, Voet D, Ramos AH, Pugh TJ, Wilkinson J, Fisher S, Winckler W, Mahan S, Ardlie K, Baldwin J, Simons JW, Kitabayashi N, MacDonald TY, Kantoff PW, Chin L, Gabriel SB, Gerstein MB, Golub TR, Meyerson M, Tewari A, Lander ES, Getz G, Rubin MA, Garraway LA. The genomic complexity of primary human prostate cancer. Nature 2011; 470(7333): 214-20.

Bhatia-Gaur R, Donjacour AA, Sciavolino PJ, Kim M, Desai N, Young P, Norton CR, Gridley T, Cardiff RD, Cunha GR, Abate-Shen C, Shen MM. Roles for Nkx3.1 in prostate development and cancer. Genes Dev 1999; 13(8): 966-977.

Biagioli MC, Hoffe SE. Emerging technologies in prostate cancer radiation therapy: improving the therapeutic window. Cancer Control 2010; 17: 223–32.

Böhnke A, Westphal F, Schmidt A, El-Awady RA, Dahm-Daphi J. Role of p53 mutations, protein function and DNA damage for the radiosensitivity of human tumor cells. Int J Radiat Biol 2004; 80(1): 53-63.

Bonkhoff H, Remberger K. Differentiation pathways and histogenetic aspects of normal and abnormal prostatic growth: A stem cell model. Prostate 1996; 28: 98–106.

Bonkhoff H. Factors implicated in radiation therapy failure and radiosensitization of prostate cancer. Prostate Cancer 2012; 2012: 593241.

Brabletz S, Brabletz T. The ZEB/miR-200 feedback loop – a motor of cellular plasticity in development and cancer? EMBO Rep 2010; 11(9): 670–677.

Bromfield GP, Meng A, Warde P, Bristow RG. Cell death in irradiated prostate epithelial cells: role of apoptotic and clonogenic cell kill. Prostate Cancer Prostatic Dis 2003; 6(1): 73-85.

Cano A, Pérez-Moreno MA, Rodrigo I, Locascio A, Blanco MJ, del Barrio MG, Portillo F, Nieto MA. The transcription factor snail controls epithelial-mesenchymal transitions by repressing E-cadherin expression. Nat Cell Biol 2000; 2(2): 76-83.

Cao Q, Yu J, Dhanasekaran SM, Kim JH, Mani RS, Tomlins SA, Mehra R, Laxman B, Cao X, Yu J, Kleer CG, Varambally S, Chinnaiyan AM. Repression of E-cadherin by the polycomb group protein EZH2 in cancer. Oncogene 2008; 27(58): 7274-84.

Chang JM, Lee HJ, Lee SE, Byun SS, Choe GY, Kim SH, Seong CK, Kim SH. Pictorial review: Unusual tumors involving the prostate: radiological-pathological findings. Br J Radiol 2008; 81(971): 907-15.

Chen W, Wang GM. Gene expression profiling of cancer stem cells in the Du145 prostate cancer cell line. Oncol Lett 2012; 3(4): 791-796.

Cheng L, Lloyd RV, Weaver AL, Pisansky TM, Cheville JC, Ramnani DM, Leibovich BC, Blute ML, Zincke H, Bostwick DG. The cell cycle inhibitors p21WAF1 and p27KIP1 are associated with survival in patients treated by salvage prostatectomy after radiation therapy. Clin Cancer Res 2000; 6(5): 1896-1899.

Chiba N, Comaills V, Shiotani B, Takahashi F, Shimada T, Tajima K, Winokur D, Hayashida T, Willers H, Brachtel E, Vivanco MD,Haber DA, Zou L, Maheswaran S. Homeobox B9 induces epithelial-to-mesenchymal transition-associated radioresistance byaccelerating DNA damage responses. Proc Natl Acad Sci U S A 2012; 109(8): 2760-5.

Choi N, Zhang B, Zhang L, Ittmann M, Xin L. Adult murine prostate basal and luminal cells are self-sustained lineages that can both serve as targets for prostate cancer initiation. Cancer Cell 2012; 21(2): 253-65.

Christiansen JJ, Rajasekaran AK. Reassessing epithelial to mesenchymal transition as a prerequisite for carcinoma invasion and metastasis. Cancer Res 2006; 66(17): 8319-26.

Collins AT, Berry PA, Hyde C, Stower MJ, Maitland NJ. Prospective identification of tumorigenic prostate cancer stem cells. Cancer Res 2005; 65: 10946–10951.

Collis SJ, Swartz MJ, Nelson WG, DeWeese TL. Enhanced radiation and chemotherapy-mediated cell killing of human cancer cells by small inhibitory RNA silencing of DNA repair factors. Cancer Res 2003; 63(7): 1550-4.

Colombel M, Eaton CL, Hamdy F, Ricci E, van der Pluijm G, Cecchini M, Mege-Lechevallier F, Clezardin P, Thalmann G. Increased expression of putative cancer stem cell markers in primary prostate cancer is associated with progression of bone metastases. Prostate 2012; 72(7): 713-20.

Colomiere M, Ward AC, Riley C, Trenerry MK, Cameron-Smith D, Findlay J, Ackland L, Ahmed N. Cross talk of signals between EGFR and IL-6R through JAK2/STAT3 mediate epithelial-mesenchymal transition in ovarian carcinomas. Br J Cancer 2009; 100(1): 134-44.

Comijn J, Berx G, Vermassen P, Verschueren K, van Grunsven L, Bruyneel E, Mareel M, Huylebroeck D, van Roy F. The two-handed E box binding zinc finger protein SIP1 downregulates E-cadherin and induces invasion. Mol Cell 2001; 7(6): 1267-78.

Conacci-Sorrell M, Simcha I, Ben-Yedidia T, Blechman J, Savagner P, Ben-Ze'ev A. Autoregulation of E-cadherin expression by cadherin-cadherin interactions: the roles of beta-catenin signalling, Slug, and MAPK. J Cell Biol 2003; 163(4): 847-57.

Culig Z. Androgen receptor cross-talk with cell signalling pathways. Growth Factors 2004; 22(3): 179–184.

de Carvalho AD, de Souza W, Morgado-Díaz JA. Morphological and molecular alterations at the junctional complex in irradiated human colon adenocarcinoma cells, Caco-2. Int J Radiat Biol 2006; 82(9): 658-68.

Deng X, Elzey BD, Poulson JM, Morrison WB, Ko SC, Hahn NM, Ratliff TL, Hu CD. Ionizing radiation induces neuroendocrine differentiation of prostate cancer cells in vitro, in vivo and in prostate cancer patients. Am J Cancer Res. 2011;1(7): 834-44. Epub 2011 Aug 18.

Dunn MW, Kazer MW. Prostate cancer overview. Semin Oncol Nurs 2011; 27(4): 241-50.

Eger A, Aigner K, Sonderegger S, Dampier B, Oehler S, Schreiber M, Berx G, Cano A, Beug H, Foisner R. DeltaEF1 is a transcriptional repressor of E-cadherin and regulates epithelial plasticity in breast cancer cells. Oncogene. 2005; 24(14): 2375-85.

English HF, Santen RJ, Isaacs JT. Response of glandular versus basal rat ventral prostatic epithelial cells to androgen withdrawal and replacement. Prostate 1987; 11: 229–242.

Germann M, Wetterwald A, Guzmán-Ramirez N, van der Pluijm G, Culig Z, Cecchini MG, Williams ED, Thalmann GN. Stem-like cells with luminal progenitor phenotype survive castration in human prostate cancer. Stem Cells. 2012; 30(6): 1076-86.

Goldstein AS, Huang J, Guo C, Garraway IP, Witte ON. Identification of a cell of origin for human prostate cancer. Science 2010; 329(5991): 568-71.

Goodison S, Urquidi V, Tarin D. CD44 cell adhesion molecules. Mol Pathol 1999; 52(4): 189-96.

Goto K, Salm SN, Coetzee S, Xiong X, Burger PE, Shapiro E, Lepor H, Moscatelli D, Wilson EL. Proximal prostatic stem cells are programmed to regenerate a proximal-distal ductal axis. Stem Cells 2006; 24(8): 1859-68.

Gravdal K, Halvorsen OJ, Haukaas SA, Akslen LA. A switch from E-cadherin to N-cadherin expression indicates epithelial to mesenchymal transition and is of strong and independent importance for the progress of prostate cancer. Clin Cancer Res 2007; 13(23): 7003-11.

Gregory PA, Bert AG, Paterson EL, Barry SC, Tsykin A, Farshid G, Vadas MA, Khew-Goodall Y, Goodall GJ. The miR-200 family and miR-205 regulate epithelial to mesenchymal transition by targeting ZEB1 and SIP1. Nat Cell Biol 2008; 10(5): 593-601.

Grünert S, Jechlinger M, Beug H. Diverse cellular and molecular mechanisms contribute to epithelial plasticity and metastasis. Nat Rev Mol Cell Biol 2003; 4(8): 657-65.

Guo C, Liu H, Zhang BH, Cadaneanu RM, Mayle AM, Garraway IP. ECaPm, CD44, and CD49f distinguish sphere-forming human prostate basal cells from a subpopulation with predominant tubule initiation capability. PLoS One 2012; 7(4): e34219.

Hajra KM, Chen DY, Fearon ER. The SLUG zinc-finger protein represses E-cadherin in breast cancer. Cancer Res. 2002; 62(6): 1613-8.

Hartwell KA, Muir B, Reinhardt F, Carpenter AE, Sgroi DC, Weinberg RA. The Spemann organizer gene, Goosecoid, promotes tumor metastasis. Proc Natl Acad Sci U S A 2006; 103(50): 18969-74.

Heidenreich A, Bolla M, Joniau S et al. European Association of Urology. Guidelines on prostate cancer. 2011. Available at: http://www.uroweb.org/gls/pdf/08_Prostate_Cancer.pdf. Accessed December 2011

Heinlein CA, Chang C. Androgen receptor in prostate cancer. Endocr Rev 2004; 25(2): 276–308.

Hensley HH, Hannoun-Levi JM, Hachem P, Mu Z, Stoyanova R, Khor LY, Agrawal S, Pollack A. PKA knockdown enhances cell killing in response to radiation and androgen deprivation. Int J Cancer. 2011; 128(4): 962-73.

Huber MA, Azoitei N, Baumann B, Grunert S, Sommer A, Pehamberger H, Kraut N, Beug H, Wirth T. NF-kB is essential for epithelial-mesenchymal transition and metastasis in a model of breast cancer progression. J Clin Invest 2004; 114(4): 569-581.

Huber MA, Kraut N, Beug H. Molecular requirements for epithelial-mesenchymal transition during tumor progression. Curr Opin Cell Biol 2005; 17(5): 548-58.

Humphrey PA. Diagnosis of adenocarcinoma in prostate needle biopsy tissue. J Clin Pathol 2007; 60(1): 35–42.

Huttner WB, Gerdes HH, Rosa P. The granin (chromogranin/secretogranin) family. Trends Biochem Sci 1991; 16(1): 27-30.

Imamichi Y, Menke A. Signalling Pathways Involved in Collagen-Induced Disruption of the E-Cadherin Complex during Epithelial-Mesenchymal Transition. Cells Tissues Organs 2007; 185(1-3): 180–190.

Isaacs JT, Coffey DS. Etiology and disease process of benign prostatic hyperplasia. Prostate Suppl 1989; 2: 33-50.

Jin RJ, Lho Y, Connelly L, Wang Y, Yu X, Saint Jean L, Case TC, Ellwood-Yen K, Sawyers CL, Bhowmick NA, Blackwell TS, Yull FE, Matusik RJ. The nuclear factor-kappaB pathway controls the progression of prostate cancer to androgen-independent growth. Cancer Res 2008; 68(16): 6762-9.

Kaighn ME, Narayan KS, Ohnuki Y, Lechner JF, Jones LW. Establishment and characterization of a human prostatic carcinoma cell line (PC-3). Invest Urol 1979; 17(1): 16-23.

Kang Y, Massague J. Epithelial-mesenchymal transitions: twist in development and metastasis. Cell 2004; 118: 277-279.

Karar J, Maity A. Modulating the tumor microenvironment to increase radiation responsiveness. Can Biol Ther 2009; 8(21): 1994–2001.

Ke XS, Qu Y, Goldfinger N, Rostad K, Hovland R, Akslen LA, Rotter V, Øyan AM, Kalland KH. Epithelial to mesenchymal transition of a primary prostate cell line with switches of cell adhesion modules but without malignant transformation. PLoS One 2008; 3(10): e3368.

Khor LY, Bae K, Paulus R, Al-Saleem T, Hammond ME, Grignon DJ, Che M, Venkatesan V, Byhardt RW, Rotman M, Hanks GE, Sandler HM, Pollack A. MDM2 and Ki-67 predict for distant metastasis and mortality in men treated with radiotherapy and androgen deprivation for prostate cancer: RTOG 92-02. J Clin Oncol 2009; 27(19): 3177-84.

Kiviharju-af Hällström TM, Jäämaa S, Mönkkönen M, Peltonen K, Andersson LC, Medema RH, Peehl DM, Laiho M. Human prostate epithelium lacks Wee1A-mediated DNA damage-induced checkpoint enforcement. Proc Natl Acad Sci U S A 2007; 104(17): 7211-6.

Kong Z, Xie D, Boike T, Raghavan P, Burma S, Chen DJ, Habib AA, Chakraborty A, Hsieh JT, Saha D. Downregulation of human DAB2IP gene expression in prostate cancer cells results in resistance to ionizing radiation. Cancer Res. 2010; 70(7): 2829-39.

Lagadec C, Vlashi E, Della Donna L, Dekmezian C, Pajonk F. Radiation-induced reprogramming of breast cancer cells. Stem Cells 2012; 30(5): 833-44.

Lee JM, Dedhar S, Kalluri R, Thompson EW. The epithelial-mesenchymal transition: new insights in signalling, development, and disease. J Cell Biol 2006; 172(7): 973-81.

Li H, Chen X, Calhoun-Davis T, Claypool K, Tang DG. PC3 human prostate carcinoma cell holoclones contain self-renewing tumor-initiating cells. Cancer Res 2008; 68(6): 1820-5.

Li T, Zeng ZC, Wang L, Qiu SJ, Zhou JW, Zhi XT, Yu HH, Tang ZY. Radiation enhances long-term metastasis potential of residual hepatocellular carcinoma in nude mice through TMPRSS4-induced epithelial-mesenchymal transition. Cancer Gene Ther 2011; 18(9): 617-26.

Li W, Katoh H, Wang L, Yu X, Du Z, Yan X, Zheng P, Liu Y. FOXP3 Regulates Sensitivity of Cancer Cells to Irradiation by Transcriptional Repression of BRCA1. Cancer Res 2013. [Epub ahead of print]

Liu AY, LaTray L, van Den Engh G. Changes in cell surface molecules associated with in vitro culture of prostatic stromal cells. Prostate 2000; 44(4): 303-12.

Locke JA, Guns ES, Lubik AA, Adomat HH, Hendy SC, Wood CA, Ettinger SL, Gleave ME, Nelson CC. Androgen levels increase by intratumoral de novo steroidogenesis during progression of castration-resistant prostate cancer. Cancer Res 2008; 68(15): 6407-15.

Locke M, Heywood M, Fawell S, Mackenzie IC. Retention of intrinsic stem cell hierarchies in carcinoma-derived cell lines. Cancer Res 2005; 65(19): 8944-50.

Long RM, Morrissey C, Fitzpatrick JM, Watson RW. Prostate epithelial cell differentiation and its relevance to the understanding of prostate cancer therapies. Clin Sci (Lond) 2005; 108(1): 1-11.

Lu X, Yang C, Hill R, Yin C, Hollander MC, Fornace AJ Jr, Van Dyke T. Inactivation of gadd45a sensitizes epithelial cancer cells to ionizing radiation in vivo resulting in prolonged survival. Cancer Res 2008; 68(10): 3579-83.

Ma L, Teruya-Feldstein J, Weinberg RA. Tumor invasion and metastasis initiated by microRNA-10b in breast cancer. Nature 2007; 449(7163): 682-8.

Mahajan K, Coppola D, Rawal B, Chen YA, Lawrence HR, Engelman RW, Lawrence NJ, Mahajan NP. Ack1-mediated androgen receptor phosphorylation modulates radiation resistance in castration-resistant prostate cancer. J Biol Chem 2012; 287(26): 22112-22.

Mani SA, Yang J, Brooks M, Schwaninger G, Zhou A, Miura N, Kutok JL, Hartwell K, Richardson AL, Weinberg RA. Mesenchyme Forkhead 1 (FOXC2) plays a key role in metastasis and is associated with aggressive basal-like breast cancers. Proc Natl Acad Sci U S A 2007; 104(24): 10069-74.

Mani SA, Guo W, Liao MJ, Eaton EN, Ayyanan A, Zhou AY, Brooks M, Reinhard F, Zhang CC, Shipitsin M, Campbell LL, Polyak K, Brisken C, Yang J, Weinberg RA. The epithelial-mesenchymal transition generates cells with properties of stem cells. Cell 2008; 133(4): 704-15.

Martin A, Cano A. Tumorigenesis: Twist1 links EMT to self-renewal. Nat Cell Biol 2010; 12(10): 924-5.

McDonnell TJ, Troncoso P, Brisbay SM, Logothetis C, Chung LW, Hsieh JT, Tu SM, Campbell ML. Expression of the protooncogene bcl-2 in the prostate and its association with emergence of androgen-independent prostate cancer. Cancer Res 1992; 52(24): 6940-4.

McPhee TR, McDonald PC, Oloumi A, Dedhar S. Integrin-linked kinase regulates E-cadherin expression through PARP-1. Dev Dyn 2008; 237(10): 2737-47.

Min J, Zaslavsky A, Fedele G, McLaughlin SK, Reczek EE, De Raedt T, Guney I, Strochlic DE, Macconaill LE, Beroukhim R, Bronson RT, Ryeom S, Hahn WC, Loda M, Cichowski K. An oncogene-tumor suppressor cascade drives metastatic prostate cancer by coordinately activating Ras and nuclear factor-kappaB. Nat Med 2010; 16(3): 286–294.

Morel AP, Lièvre M, Thomas C, Hinkal G, Ansieau S, Puisieux A. Generation of breast cancer stem cells through epithelial-mesenchymal transition. PLoS One. 2008 Aug 6; 3(8): e2888.

Mottet N, Bellmunt J, Bolla M, Joniau S, Mason M, Matveev V, Schmid HP, Van der Kwast T, Wiegel T, Zattoni F, Heidenreich A. EAU guidelines on prostate cancer. Part II: Treatment of advanced, relapsing, and castration-resistant prostate cancer. Eur Urol 2011; 59(4): 572-83.

Mouraviev V, Polascik TJ. Update on cryotherapy for prostate cancer in 2006. Curr Opin Urol 2006; 16: 152-156.

Murali AK, Norris JS. Differential expression of epithelial and mesenchymal proteins in a panel of prostate cancer cell lines. J Urol 2012; 188(2): 632-8.

Niciforovic A, Djordjevic J, Adzic M, Vucic V, Mitrasinovic PM, Radojcic MB. Experimental and systems biology studies of the molecular basis for the radioresistance ofprostate carcinoma cells. Ann Biomed Eng 2008; 36(5): 831-8.

Onder TT, Gupta PB, Mani SA, Yang J, Lander ES, Weinberg RA. Loss of E-cadherin promotes metastasis via multiple downstream transcriptional pathways. Cancer Res 2008; 68(10): 3645-54.

Oudard S. Progress in emerging therapies for advanced prostate cancer. Cancer Treat Rev 2013; 39(3): 275-89.

Ozdamar B, Bose R, Barrios-Rodiles M, Wang HR, Zhang Y, Wrana JL. Regulation of the polarity protein Par6 by TGFbeta receptors controls epithelial cell plasticity. Science 2005; 307(5715): 1603-9.

Palafox M, Ferrer I, Pellegrini P, Vila S, Hernandez-Ortega S, Urruticoechea A, Climent F, Soler MT, Muñoz P, Viñals F, Tometsko M, Branstetter D, Dougall WC,González-Suárez E. RANK induces epithelial-mesenchymal transition and stemness in human mammary epithelial cells and promotes tumorigenesis and metastasis. Cancer Res 2012; 72(11): 2879-88.

Park CC, Henshall-Powell RL, Erickson AC, Talhouk R, Parvin B, Bissell MJ, Barcellos-Hoff MH. Ionizing radiation induces heritable disruption of epithelial cell interactions. Proc Natl Acad Sci U S A 2003; 100(19): 10728-33.

Perez-Moreno MA, Locascio A, Rodrigo I, Dhondt G, Portillo F, Nieto MA, Cano A. A new role for E12/E47 in the repression of E-cadherin expression and epithelial-mesenchymal transitions. J Biol Chem 2001; 276(29): 27424-31.

Pollack A, Bae K, Khor LY, Al-Saleem T, Hammond ME, Venkatesan V, Byhardt RW, Asbell SO, Shipley WU, Sandler HM. The importance of protein kinase A in prostate cancer: relationship to patient outcome in Radiation Therapy Oncology Group trial 92-02. Clin Cancer Res. 2009; 15(17): 5478-84.

Quinn DI, Henshall SM, Sutherland RL. Molecular markers of prostate cancer outcome. Eur J Can 2005; 41(6): 858–887.

Radisky DC, Levy DD, Littlepage LE, Liu H, Nelson CM, Fata JE, Leake D, Godden EL, Albertson DG, Nieto MA, Werb Z, Bissell MJ. Rac1b and reactive oxygen species mediate MMP-3-induced EMT and genomic instability. Nature 2005; 436(7047): 123-7.

Rashid A, Liu C, Sanli T, Tsiani E, Singh G, Bristow RG, Dayes I, Lukka H, Wright J, Tsakiridis T. Resveratrol enhances prostate cancer cell response to ionizing radiation. Modulation of the AMPK, Akt and mTOR pathways. Radiat Oncol 2011; 6: 144.

Roach M 3rd, Waldman F, Pollack A. Predictive models in external beam radiotherapy for clinically localized prostate cancer. Cancer 2009; 115(13 Suppl): 3112-20.

Rogakou EP, Pilch DR, Orr AH, Ivanova VS, Bonner WM. DNA double-stranded breaks induce histone H2AX phosphorylation on serine 139. J Biol Chem 1998; 273(10): 5858-68.

Ross JS, Kallakury BV, Sheehan CE, Fisher HA, Kaufman RP Jr, Kaur P, Gray K, Stringer B. Expression of nuclear factor-kappa B and I kappa B alpha proteins in prostatic adenocarcinomas: correlation of nuclear factor-kappa B immunoreactivity with disease recurrence. Clin Cancer Res 2004; 10(7): 2466-72.

Rosser CJ, Reyes AO, Vakar-Lopez F, Levy LB, Kuban DA, Hoover DC, Lee AK, Pisters LL. Bcl-2 is significantly overexpressed in localized radio-recurrent prostate carcinoma, compared with localized radio-naive prostate carcinoma. Int J Radiat Oncol Biol Phys 2003; 56(1): 1-6.

Sanli T, Rashid A, Liu C, Harding S, Bristow RG, Cutz JC, Singh G, Wright J, Tsakiridis T. Ionizing radiation activates AMP-activated kinase (AMPK): a target for radiosensitization of human cancer cells. Int J Radiat Oncol Biol Phys 2010; 78(1): 221-9

Sartor AO, Fitzpatrick JM. Urologists and oncologists: adapting to a new treatment paradigm in castration-resistant prostate cancer (CRPC). BJU Int 2012; 110(3): 328-35.

Serafin AM, Akudugu JM, Böhm L. Studies on the influence of DNA repair on radiosensitivity in prostate cell lines. Urol Res. 2003; 31(4): 227-31.

Shaheen FS, Znojek P, Fisher A, Webster M, Plummer R, Gaughan L, Smith GC, Leung HY, Curtin NJ, Robson CN. Targeting the DNA double strand break repair machinery in prostate cancer. PLoS One. 2011; 6(5): e20311.

Schaue D, McBride WH. Counteracting tumor radioresistance by targeting DNA repair. Mol Cancer Ther 2005; 4(10): 1548-50.

Signoretti S, Waltregny D, Dilks J, Isaac B, Lin D, Garraway L, Yang A, Montironi R, McKeon F, Loda M. p63 is a prostate basal cell marker and is required for prostate development. Am J Pathol 2000; 157: 1769 – 1775.

Skvortsova I, Skvortsov S, Stasyk T, Raju U, Popper BA, Schiestl B, von Guggenberg E, Neher A, Bonn GK, Huber LA, Lukas P. Intracellular signalling pathways regulating radioresistance of human prostate carcinoma cells. Proteomics. 2008; 8(21): 4521-33.

Sobrado VR, Moreno-Bueno G, Cubillo E, Holt LJ, Nieto MA, Portillo F, Cano A. The class I bHLH factors E2-2A and E2-2B regulate EMT. J Cell Sci 2009; 122(Pt 7): 1014-24.

Spaderna S, Schmalhofer O, Wahlbuhl M, Dimmler A, Bauer K, Sultan A, Hlubek F, Jung A, Strand D, Eger A, Kirchner T, Behrens J, Brabletz T. The transcriptional repressor ZEB1 promotes metastasis and loss of cell polarity in cancer. Cancer Res 2008; 68(2): 537-44.

Stone KR, Mickey DD, Wunderli H, Mickey GH, Paulson DF. Isolation of a human prostate carcinoma cell line (DU 145). Int J Cancer 1978; 21(3): 274-81.

Stoyanova R, Hachem P, Hensley H, Khor LY, Mu Z, Hammond ME, Agrawal S, Pollack A. Antisense-MDM2 sensitizes LNCaP prostate cancer cells to androgen deprivation, radiation, and the combination in vivo. Int J Radiat Oncol Biol Phys 2007 Jul 15; 68(4): 1151-60.

Strauss R, Hamerlik P, Lieber A, Bartek J. Regulation of stem cell plasticity: mechanisms and relevance to tissue biology and cancer. Mol Ther 2012; 20(5): 887-97.

Strauss R, Li ZY, Liu Y, Beyer I, Persson J, Sova P, Möller T, Pesonen S, Hemminki A, Hamerlik P, Drescher C, Urban N, Bartek J, Lieber A. Analysis of epithelial and mesenchymal markers in ovarian cancer reveals phenotypic heterogeneity and plasticity. PLoS One. 2011; 6(1): e16186.

Sugrue T, Brown JA, Lowndes NF, Ceredig R. Multiple facets of the DNA damage response contribute to the radioresistance of mouse mesenchymal stromal cell lines. Stem Cells 2013; 31(1): 137-45.

Tavazoie SF, Alarcón C, Oskarsson T, Padua D, Wang Q, Bos PD, Gerald WL, Massagué J. Endogenous human microRNAs that suppress breast cancer metastasis. Nature 2008; 451(7175): 147-52.

Taylor BS, Schultz N, Hieronymus H, Gopalan A, Xiao Y, Carver BS, Arora VK, Kaushik P, Cerami E, Reva B, Antipin Y, Mitsiades N, Landers T, Dolgalev I, Major JE, Wilson M, Socci ND, Lash AE, Heguy A, Eastham JA, Scher HI, Reuter VE, Scardino PT, Sander C, Sawyers CL, Gerald WL. Integrative genomic profiling of human prostate cancer. Cancer Cell 2010; 18(1): 11-22.

Taylor RA, Toivanen R, Frydenberg M, Pedersen J, Harewood L, Australian Prostate Cancer Bioresource, Collins AT, Maitland NJ, Risbridger GP. Human epithelial basal cells are cells of origin of prostate cancer, independent of CD133 status. Stem Cells 2012; 30(6): 1087-96.

Theys J, Jutten B, Habets R, Paesmans K, Groot AJ, Lambin P, Wouters BG, Lammering G, Vooijs M. E-Cadherin loss associated with EMT promotes radioresistance in human tumor cells. Radiother Oncol 2011; 99(3): 392-7.

Thiery JP, Sleeman JP. Complex networks orchestrate epithelial-mesenchymal transitions. Nat Rev Mol Cell Biol 2006; 7(2): 131-42.

Tomlins SA, Laxman B, Dhanasekaran SM, Helgeson BE, Cao X, Morris DS, Menon A, Jing X, Cao Q, Han B, Yu J, Wang L, Montie JE, Rubin MA, Pienta KJ, Roulston D, Shah RB, Varambally S, Mehra R, Chinnaiyan AM. Distinct classes of chromosomal rearrangements create oncogenic ETS gene fusions in prostate cancer. Nature 2007; 448(7153): 595-9.

Tsujimura A, Koikawa Y, Salm S, Takao T, Coetzee S, Moscatelli D, Shapiro E, Lepor H, Sun TT, Wilson EL. Proximal location of mouse prostate epithelial stem cells: a model of prostatic homeostasis. J Cell Biol 2002; 157(7): 1257-65.

Tu S, Lin S. Prostate Cancer Stem Cells. Clin Gen Can 2012; 10(2): 69-76.

van Bokhoven A, Varella-Garcia M, Korch C, Johannes WU, Smith EE, Miller HL, Nordeen SK, Miller GJ, Lucia MS. Molecular characterization of human prostate carcinoma cell lines. Prostate 2003; 57(3): 205-25.

van Leenders G, Dijkman H, Hulsbergen-van de Kaa C, Ruiter D, Schalken J. Demonstration of intermediate cells during human prostate epithelial differentiation in situ and in vitro using triple-staining confocal scanning microscopy. Lab Invest 2000; 80(8): 1251-8.

Verhagen AP, Aalders TW, Ramaekers FC, Debruyne FM, Schalken JA. Differential expression of keratins in the basal and luminal compartments of rat prostatic epithelium during degeneration and regeneration. Prostate 1988; 13(1): 25-38.

Verhagen AP, Ramaekers FC, Aalders TW, Schaafsma HE, Debruyne FM, Schalken JA. Colocalization of basal and luminal cell-type cytokeratins in human prostate cancer. Cancer Res 1992; 52(22): 6182–6187.

Vucić V, Isenović ER, Adzić M, Ruzdijić S, Radojcić MB. Effects of gamma-radiation on cell growth, cycle arrest, death, and superoxide dismutase expression by DU 145 human prostate cancer cells. Braz J Med Biol Res 2006; 39(2): 227-36.

Wang X, Zheng M, Liu G, Xia W, McKeown-Longo PJ, Hung MC, Zhao J. Krüppel-like factor 8 induces epithelial to mesenchymal transition and epithelial cell invasion. Cancer Res 2007; 67(15): 7184-93.

Wang X, Ma Z, Xiao Z, Liu H, Dou Z, Feng X, Shi H. Chk1 knockdown confers radiosensitization in prostate cancer stem cells. Oncol Rep 2012; 28(6): 2247-54.

Webber MM, Bello D, Quader S. Immortalized and tumorigenic adult human prostatic epithelial cell lines: characteristics and applications Part 2. Tumorigenic cell lines. Prostate 1997; 30(1): 58-64.

Weiss L. Cancer cell heterogeneity. Cancer Metastasis Rev 2000; 19: 345–50.

Wolff JM, Mason M. Drivers for change in the management of prostate cancer - guidelines and new treatment techniques. BJU Int 2012; 109 Suppl 6: 33-41.

Xiao W, Graham PH, Power CA, Hao J, Kearsley JH, Li Y. CD44 is a biomarker associated with human prostate cancer radiation sensitivity. Clin Exp Metastasis 2012; 29(1): 1-9.

Xin L. Cells of origin for cancer: an updated view from prostate cancer. Oncogene 2013; 32(32): 3655-63

Yamamoto H, Masters JR, Dasgupta P, Chandra A, Popert R, Freeman A, Ahmed A. CD49f is an efficient marker of monolayer- and spheroid colony-forming cells of the benign and malignant human prostate. PLoS One 2012; 7(10): e46979.

Yamashita S, Miyagi C, Fukada T, Kagara N, Che YS, Hirano T. Zinc transporter LIVI controls epithelial-mesenchymal transition in zebrafish gastrula organizer. Nature 2004; 429: 298-302.

Yang J, Mani SA, Donaher JL, Ramaswamy S, Itzykson RA, Come C, Savagner P, Gitelman I, Richardson A, Weinberg RA. Twist, a master regulator of morphogenesis, plays an essential role in tumor metastasis. Cell 2004; 117(7): 927-39.

Yang J, Weinberg RA. Epithelial-mesenchymal transition: at the crossroads of development and tumor metastasis. Dev Cell 2008; 14(6): 818-29.

Yoshioka Y. Current status and perspectives of brachytherapy for prostate cancer. Int J Clin Oncol 2009; 14: 31-36.

Yu C, Yao Z, Jiang Y, Keller ET. Prostate cancer stem cell biology. Minerva Urol Nefrol 2012; 64(1): 19-33.

Zavadil J, Cermak L, Soto-Nieves N, Böttinger EP. Integration of TGF-beta/Smad and Jagged1/Notch signalling in epithelial-to-mesenchymal transition. EMBO J 2004; 23(5): 1155-65.

Zellweger T, Chi K, Miyake H, Adomat H, Kiyama S, Skov K, Gleave ME. Enhanced radiation sensitivity in prostate cancer by inhibition of the cell survival protein clusterin. Clin Cancer Res 2002; 8(10): 3276-84.

Zhou BP, Deng J, Xia W, Xu J, Li YM, Gunduz M, Hung MC. Dual regulation of Snail by GSK-3b-mediated phosphorylation in control of epithelial-mesenchymal transition. Nat Cell Biol 2004; 6:931-940.

Zhu ML, Kyprianou N. Androgen receptor and growth factor signalling cross-talk in prostate cancer cells. Endocr Rel Can 2008; 15(4): 841–849.

Zoltan-Jones A, Huang L, Ghatak S, Toole BP. Elevated hyaluronan production induces mesenchymal and transformed properties in epithelial cells. Biol Chem 2003; 278(46): 45801-10.